AN INVESTIGATION OF THE EFFECTIVENESS OF BAFFLES IN PROMOTING MIXING OF A HOT GAS WITH COLD AIR UNDER STEADY FLOW CONDITIONS.

Charles W. Ulrich

AN INVESTIGATION OF THE EFFECTIVENESS OF BAFFLES IN PROMOTING MIXING OF A HOT GAS WITH COLD AIR UNDER STEADY FLOW CONDITIONS

A Thesis

Submitted to the Graduate Faculty

of the University of Minnesota

by

Charles W. Ullrich

Lt., U.S. Navy

In Partial Fulfillment of the Requirements

for the Degree of

Master of Science in Aeronautical Engineering

June 1952

ACKNOWLEDGMENTS

Expressions of gratitude are sincerely due to many members of the Mechanical and Aeronautical Engineering Departments, of the University of Minnesota, for their generous aid and support in the prosecution of this investigation.

In particular, the author wishes to express thanks to Dr. Newman A. Hall and Professor Thomas E. Murphy, for their help and advice; to Robert Robarge, for his aid in construction of the wing baffles; to Michael Shonberg and William Alden, for their patience with an amateur machinist; and to Dorothy Ullrich, for moral support, so often needed in the preparation of this Thesis.

TABLE OF CONTENTS

TABLE OF CONTENTS CONTINUED

LIST OF FIGURES

LIST OF FIGURES CONTINUED

LIST OF TABLES

SUMMARY

An experimental investigation of the relative effectiveness of several baffle types in promoting velocity and temperature mixing of a cold air stream concentric with a hot gas stream, has been conducted. Based on a ratio of centerline mixing attained to pressure drop resulting, only one baffle type, that of stub wings projecting into the mixing chamber, proved more effective than a no-baffle configuration. Ignoring pressure losses, however, screen-type baffles produced better velocity mixing, but very poor temperature mixing.

Based on velocity potential core lengths (the axial distance the hot central gas maintains its initial velocity) and comparing with known results for isothermal velocity mixing, the effect of compressibility, contrary to other investigators, appears to be an improvement in velocity mixing.

That temperature diffuses more rapidly than velocity, when baffles do not obstruct the flow, a conclusion reached by several other experimentors, is verified by the single baffleless configuration tested.

The investigation was conducted under the auspices of the Mechanical and Aeronautical Engineering Departments of the University of Minnesota in partial fulfillment of the requirements for the degree of Master of Science.

LIST OF SYMBOLS

D	Diameter of primary jet nozzle, inches.
L	Value of X/D for end of potential core.
p	Static pressure, inches of water.
q	Dynamic pressure, inches of water, $= \frac{1}{2}\rho V^2$
r	Radial distance from jet axis, inches.
r_m	Radius at which V (or T) is halfway between V (or T) at axis and that of secondary stream.
T	Temperature, $^{o}F.$, at any point in mixing region.
T_c	Temperature, ^{o}F, on axis, at a given X.
T_p	Temperature, ^{o}F, of primary stream at X = 0.
T_{pO}	Temperature, $^{o}F.$ upstream of primary orifice plate.
T_{sO}	Temperature, ^{o}F, upstream of secondary orifice plate.
u	Time-average velocity in axial direction at any point. $\frac{ft.}{sec.}$
u_c	Velocity on axis at a given X, ft./sec.
u_p	Centerline velocity of primary stream at X = 0, ft./sec.
u_s	Velocity of undisturbed secondary stream, ft./sec.
X	Axial distance downstream from nozzle exit, inches.
Y	Lateral distance from nozzle centerline, inches.
λ	Velocity ratio $= u_s/u_p$.
ΔP_p	Pressure drop across primary flow orifice, inches water.
ΔP_s	Pressure drop across secondary flow orifice, inches water.

INTRODUCTION

Proper mixing of fluids under various conditions is important in that the design of such items as combustion chambers, mixing tanks, jet pumps, and thrust augmenters, depend to a great extent on obtaining or preventing mixing of fluids. In particular, according to Godsey and Young (Ref. 1):

> Although nonuniformity of temperature distribution may have only small effect upon cycle efficiency, it is essential that good mixing be obtained in order to avoid undesirable stratification in the gas flow entering the turbine blading. Excessive stratification can result in local hot spots in which permissible temperature limits may be exceeded by several hundred degrees.

According to Ref. 2, the mixing of gas streams can be accomplished by several methods as follows:

(A) Mixing by molecular diffusion across boundaries of the streams. (Laminar Flow).

(B) Mixing by random turbulence.

(C) Mixing by induced turbulence:

- (1) Baffles or obstructions in joined streams.
- (2) Cross flow of streams.
- (3) Stirring jet.
- (4) Interleafing.
- (5) Elbow in joined streams.

Of the above, (A) is far too slow to be of practical significance in combustion chamber work, and (B), while eventually

effective and considerably faster than (A), would require an excessively long secondary zone. (C), while most rapid and effective, involves larger pressure losses than either of the other two. Some phases of (C) are amenable to analytical solution: the pressure losses associated with the mixing of the two streams are functions of the momenta of the streams, but the penetration and mixing of a cold air stream into a hot stream introduces density and other property changes in the fluid which complicate the problem.

Numerous investigators have studied the problem of mixing from both the theoretical and experimental viewpoint; various combinations of the variables involved in mixing, such as initial temperatures, initial velocities, with or without secondary moving streams, turbulence levels, and "turbulence promoters" have been utilized in tests.

According to Ferrari (Ref. 3), the important concept of mixing length, l, is analogous to the molecular mean free path in the kinetic gas theory. Mixing length l may be defined as the path normal to the lines of flow which the particles can trace out and still maintain their individuality, i.e., without assuming the physical characteristics of the medium in which they are immersed. Prandtl and his associates assume that throughout the path l each fluid particle maintains its momentum. Taylor objects however, and says that the instantaneous pressure differences may cause the

velocity of displaced particles to vary, and therefore it is more logical to assume that it is the vorticity, upon which the instantaneous pressure distributions have no effect, that is maintained constant.

Shapiro and Forrestal (Ref. 4) and Cleeves and Boelter, (Ref. 5) present excellent tabular summaries of the theoretical and experimental work accomplished in the fluid mixing problem. Squire (Ref. 6) has outlined the various theoretical approaches to the mixing problem. Forrestal and Shapiro based their "Momentum and Mass Transfer in Coaxial Gas Jets" (Ref. 4) on the work of Squire and Trouncer (Ref. 7), and arrived at several important results and semi-empirical equations to define the mixing zone.

Stanley Corrsin has prepared several papers on the study of jet flow, utilizing a primary flow in motion but a stationary receiving fluid, temperature and velocity profiles being obtained. (Refs. 8, 9, and 10). He concludes that temperature diffuses more rapidly than velocity. (Ref. 8). That heat diffuses more rapidly than velocity is verified on a qualitative basis by the modified vorticity-transfer theory, whereas the momentum transfer approach produces identical curves for velocity and temperature distributions.

A recent investigation by Ruegg and Klug (Ref. 11), that included an experimental study of the temperature mixing of primary flame gas and secondary air, produced several interesting conclusions. Ruegg and Klug found, in general, a constant potential core length

for temperature, regardless of velocity ratio. They also indicate that the effect of compressibility is to retard mixing. In addition, verification of the faster diffusion of temperature in comparison to velocity is found.

The effect of various baffles placed in the streams of moving gases in order to induce turbulence to promote mixing has also been investigated to some extent. (Ref. 12, 13, 14, 15, 16, 17). The California Institute of Technology conducted several experiments to determine the mixing resulting from the use of variously shaped holes to introduce secondary air into the primary stream in a combustion chamber. It was found that slight changes in the shape of the holes reduced pressure drop across the holes about thirty percent without any appreciable effect on the mixing (Ref. 17 and 18). Folsom and Ferguson (Ref. 14) found that a propeller was more effective than jets in promoting mixing of liquids in a large tank. A. L. Larson (Ref. 12) found that a spiral placed in refrigerant evaporator coils, when using Freon 12 as the fluid, produced turbulence, to cause accelerated heat transfer, with a lower pressure drop than other types of baffles tested. The same result had previously been found by Seigel when a liquid was used as the fluid (Ref. 13).

Thus it may be seen from this brief introduction that the mixing and turbulence problem is not an untouched one: on the contrary, the ample literature on the subject, with many

investigators seemingly in disagreement with results of other investigators, indicates that experimental means must generally be utilized to predict adequate mixing, with as short a mixing chamber length as possible, and with minimum pressure drop.

This latter statement, then, broadly defines the problem studied in this experiment. In particular, the relative effectiveness of various baffle arrangements in promoting mixing of a hot gas with cold air, under steady flow conditions, is investigated by means of temperature and velocity surveys of the mixing region.

EQUIPMENT

GENERAL DESCRIPTION

Figure 1 is a schematic diagram of the apparatus used in this investigation. Photographs of the equipment components are Figures 2a to 2f, inclusive.

The apparatus consisted of a dual air supply system capable of supplying air to primary and secondary lines. Measurement of the two mass rates of air flow was accomplished through standard A.S.M.E. square-edged orifices with radius pressure taps, in accordance with Ref. 19.

The primary flow, supplied by the building air compressor system, passed through a two inch standard pipe to a rectangular $3\frac{3}{4}$" by $4\frac{1}{4}$" stainless steel "heater box" which was supplied with acetylene gas for combustion in the excess primary air in order to heat the primary air. The heated excess air and products of combustion left the heater box through a small section of two inch pipe which was then reduced to a one inch inside diameter pipe through a standard 90 degree reducing elbow. The one inch line then passed through a small circular "adapter" tank, one end of which was connected to the round secondary air flow line and the other end to the square pre-test section. The primary line then ejected into the center of the test section as a free jet.

The secondary air, supplied by an engine driven compressor in the test cell, exited from the compressor through a manifold to a 6" diameter pipe which was bolted to the circular adapter tank. The air then exited from the adapter tank to the square pre-test section where an 18 mesh wire screen was placed across the flow (and around the primary line) in order to assure as uniform a turbulence distribution (isotropic) as possible. The secondary air then flowed into the square test section, surrounding and concentric with the primary air.

It should be noted that although two small turnbuckles to support and adjust the primary pipe were located about one inch downstream of the wire screen, there were no obstructions to the flow of primary or secondary air for a distance of about 13 inches prior to the test section zero point, located at the end of the primary line. A six degree taper on the outside wall of the primary line at its free end, was used to prevent excessive separation, with resultant eddies in the flow, as the secondary air passed by the end of the primary pipe.

The test section itself consisted of a six inch square cross-section, 7 ft. 4 inch long duct, constructed on three sides of 16 gauge sheet metal, and on the fourth side of twelve inch long, 18 gauge sheet metal sliding panels, which rode in grooves to give a tight fit. This sliding panel arrangement was necessary in order to longitudinally position the four inch long sheet metal

measuring plate, which contained a total head tube, static pressure tap, and an iron-constantan thermocouple, in the test section as desired. The usable length of the test section (from the point where the primary line ended to the duct exit) was 73 inches. The end of the duct was open, but a large sheet metal "funnel" effectively collected the warm gases and passed them to an exhaust manifold to be handled by the test cell exhaust system.

THE AIRFLOW SYSTEM

The primary air was supplied by permanent compressor installations located in the Mechanical Engineering Building. The basement unit stored air in a 30 ft.^{3} tank at a pressure of 100 psi., and the smaller dynamometer room unit supplemented the basement supply when the pressure dropped below 80 psi. Control of the primary air was accomplished by use of a gate valve located upstream of the heater box and primary measuring orifice. An extension on the valve handle permitted control to be exercised at the test section itself.

The secondary air was obtained from a permanent installation located in the turbine test cell of the Mechanical Engineering Department. A gasoline powered Lycoming Model O-435-F air cooled Army tank engine, rated at 162 H.P. at 2800 r.p.m., drives a centrifugal compressor. The compressor is a 7.48:1 gear ratio supercharger taken from an Allison V-1710 Aircraft engine.

Blower speed can be accurately controlled by throttling the engine. (See Fig. 2a).

An iron-constantan thermocouple and a standard A.S.M.E. square-edged orifice is mounted upstream of the blower inlet to permit mass rate air flow calculations.

HEATING UNIT

The furnishing of an adequate and dependable supply of heat for the primary air turned out to be a problem. At first it was desired to use electrical energy to heat the air so that products of combustion would not be one of the mixing gases and because this source of heat is easier and cleaner to handle. Hence, two different 220 volt electrical heating units were constructed, one using nichrome wire "Glo-Coils" across the flow and the other using individual nichrome wire coils in hollow porcelain tubes parallel with the flow, both units consisting of ten circuits connected in parallel. Both units burned out after about ten minutes operation at the required primary mass flow rates. The nichrome wire itself burned or broke in both cases. Sufficient data was not obtained using the electrical heaters and all data reported herein was obtained using a combustion type heater.

It was decided that, in view of the limited experimental accuracy possible with the equipment available, there would be no significant errors introduced into the investigation by using hot

gases of combustion with excess air as primary flow, instead of just pure heated air. Hence a combustion type heater box was designed and constructed. See Fig. 2b. A fourteen inch long stainless steel box of $3\frac{3}{4}$ in. by $4\frac{1}{4}$ in. rectangular cross section was flanged and coupled into the primary line downstream of the primary measuring orifice. A 3/8 inch steel pipe was inserted across the heater box, one end being connected to an acetylene supply line and the protruding end being capped. Five 0.0520 inch diameter holes, one inch apart, were drilled in the downstream side of the fuel pipe to admit the gas. Ignition of the acetylene-air mixture was accomplished by a Hi-Voltage Harness Tester (P.W.A. 2687) operated sparkplug, the spark gap being located 3 inches downstream and level with the center fuel hole. Besides the high and low pressure valves and pressure gages on the acetylene tank itself, located outside the test cell, there were two other valves on the acetylene line. One, a solenoid operated valve, was located at the tank engine control panel, and the other, a hand operated valve in the copper acetylene line, was located at the test section for emergency use only.

Combustion in the heater box appeared excellent, and the temperature used in the experiment was by no means the maximum possible. A temperature of 500 to 550 degrees Fahrenheit for the primary air at the beginning of the mixing region was chosen as a compromise between the need for lower temperatures for ease in

handling test equipment, and the need for a temperature hot enough to give good measurable temperature differences between primary and secondary air, at the beginning of the mixing region. Acetylene mass flow was estimated to be about 1/400 of primary air flow.

INSTRUMENTATION

The total pressure in the test section was measured by a 0.028 inch O.D. total head tube of the Kiel type, which had a Venturi shield surrounding the tube tip to insure flow normal to the 0.017 I.D. tube opening. The pitot tube shaft was a $\frac{1}{4}$ inch O.D. brass tube which was mounted in an 18 gage four inch wide sheet metal sliding panel through a leakproof packing gland. The panel also contained a 1/8 inch static pressure orifice.

To simultaneously measure the temperature and the total pressure at any chosen point, it was necessary to use B. and S. 30 gage iron-constantan thermocouple wire. A small hole was drilled in the pitot shaft about one inch from the Kiel tube end, and another hole was drilled in a small piece of copper tubing soldered onto the outer end of the shaft. A very small thermocouple bead was made on the inner end of the thermocouple wires (using a mercury pool electrical resistance method) and the bead was dipped in molten silver to possibly reduce radiation losses. The ends of the thermocouple wire were then led into the upper drilled hole, through the pitot shaft, and back out the lower hole. After

positioning the bead directly behind but about $\frac{1}{2}$ inch downstream of the rear of the Venturi shield, the two lead in holes on the shaft were carefully cemented with Sauereisen electric resistor paste cement number 78 to prevent any air leakage. The thermocouple leads were run to a rotary thermocouple switch at the test cell control panel.

Rubber and copper tubing carried the total pressure from the Kiel tube shaft to one side of a water-filled well-type manometer located at the control panel. The static pressure tap was led to a valve at the control panel which, in one position, placed static pressure in the test section on the other side of the manometer mentioned above, so that the dynamic pressure "q" was available; the static pressure valve in the second position put static pressure on one side of an inclined water-filled manometer, the other side being open to the atmosphere. Thus, total static, or dynamic pressures were available for any position of the measuring probe. The static pressure was assumed constant across the test section at any point, in accordance with accepted theory and practice. Readings obtained with the test Kiel tube were checked against readings obtained by a larger, unobstructed tube, and agreement was satisfactory.

The primary air was metered by an A.S.M.E. standard square edged orifice plate located between a 90° elbow following the gate valve and the heater box. The diameter of the orifice

was machined to 1.018 inches, giving a ratio of orifice diameter to pipe diameter of 0.508 inches. One-fourth inch radius taps for measuring the pressure drop Δp across the orifice were in accordance with A.S.M.E. standards. An iron-constantan thermocouple was inserted 47 inches upstream of the orifice. Copper tubing was used to connect the pressure taps across a water filled well type manometer, and the upstream tap was also connected to a mercury filled well-type manometer to provide upstream static pressure measurements. These two manometers were located in the test cell, near the test section, so that the primary air could be kept at a desired flow rate by the operator at the test section. See Fig. 2c. The thermocouple leads were led out to the rotary switch at the control panel.

Secondary air was also metered by an A.S.M.E. standard square edged orifice plate with radius taps and an iron-constantan thermocouple. This orifice diameter measures 5.600 inches, and, located in an eight inch diameter duct, the diameter ratio is 0.7. This orifice plate is a permanent installation for the blower and was already in place. The pressure drop across the orifice was measured on a well-type water filled manometer located at the control panel. The thermocouple leads were also led to the rotary switch at the panel.

One other iron-constantan thermocouple was made and used to measure the primary air temperature at a point about

35 inches upstream of the beginning of the mixing region. This temperature reading was necessary in order to monitor the operation of the heater unit. It was this thermocouple, in fact, that first gave indications of the approaching failure of the two discarded electrical heater units. The leads from this thermocouple were also taken to the rotary switch at the control panel.

A Leeds and Northrup Potentiometer Indicator was connected to the rotary switch at the panel, and temperatures, in degrees Fahrenheit, were read directly on the indicator according to the chosen switch position. The low scale, with divisions for each two degrees of temperature, was used for all readings below 500° F. See Fig. 2d.

BAFFLES

A total of three baffling systems were made and placed at various positions in the mixing region. See Fig. 2e

The airfoil baffle system consisted of four hand-made stub wings, chord of one inch, span of $2\frac{1}{3}$ inches, Clark-Y section, no twist or taper, rectangular tips, and made of stainless steel with a $\frac{3}{8}$ in. thick flange at one end for mounting. The wings were mounted at an angle of attack of 10° in a square steel bracket ($1\frac{1}{2}$ in. wide and $\frac{1}{8}$ in. thick) that just fit the perimeter of the test section. The chord lines were parallel with the flow, and

the free tips of the wings were long enough to just meet the extended boundary of the one inch primary pipe. See Fig. 2f. The chosen angle of attack was a compromise between the necessity for large angle for high lift and hence large tip vortices to promote mixing, and the need for low angle of attack for small drag, and consequently less pressure drop across the baffle. Screws were used to secure the bracket in the test section at three different positions. The upstream edges of the 1/8 inch thick bracket were slightly rounded so that as little disturbance as possible would be caused by the bracket itself.

The screen baffling system consisted of two layers of 18 mesh copper wire screening, mounted on either side of the square bracket used for the airfoil system. Thus, in effect, screening was placed across the mixing region at two points, 1½ inches apart, for each of the three positions of the baffle system.

The third baffle system was a combination of the two described above, the screens being placed around the bracket after the wings were mounted in the bracket.

A small slot was made on one side of the bracket and in a small section of the screen to permit the measuring probe to pass to either side of the baffle system.

The longitudinal positions of the baffles as reported herein (one, four and seven inches from the beginning of the

mixing region) refer to the position of the center line of the baffle bracket.

MISCELLANEOUS APPARATUS

In order to define the centerline of primary flow throughout the test section, a small diameter steel wire was secured about 35 inches upstream of the primary pipe exit, and extended throughout the test section to its open end. One post of a six volt battery was connected to the upstream end of the wire (inside the primary pipe) and the other post was connected, when needed, to the total head tube shaft. The wire was so centered that when the Venturi shield of the tube touched the wire, the circuit would be closed and light a six volt lamp, indicating a centered lateral position of the total head tube. Calibrations every 0.2 inch on a positioning plate then permitted lateral placement of the measuring tube with its attached thermocouple.

Limited adjustment of the test section itself about the center line of primary flow was made possible by the several test section duct supports. Limited vertical movement of the total head tube shaft for adjustment to the center line, as indicated by the six volt lamp, was accomplished by slotting the opening in the measuring panel and allowing a smaller outer plate, which held the packing gland and its pitot tube, to move up or down. The static pressure tap remained fixed in the four inch sliding panel.

Sound powered telephone headsets enabled the operator at the test section to communicate with the control panel operator.

PROCEDURE

GENERAL

After the equipment had been made and assembled, joints and fittings were tested for leaks. The manometers were checked, and the fluid levels held steady under a constant pressure.

In order to examine for leaks in the primary piping with its heater box, a rubber cork was inserted in the end of the primary line and the gate valve opened; there was negligible pressure drop across the primary measuring orifice even at upstream pressure values higher than that to be used during the tests. Hence it was concluded that the flow rates calculated from the measuring orifice would not have to be corrected for losses.

The primary orifice plate, being newly constructed for this experiment, was checked for reliability by comparing velocities at the primary pipe exit: the velocities, as calculated from center-line dynamic pressure readings at the primary exit, were checked against the velocities that should exist if the mass flows, as found from the primary orifice readings, were correct. The agreement was within 0.3 percent at the higher velocities and mass flow rates used in the actual investigation, and within 2.7 percent at lower velocities and mass flow rates. It should be noted that this orifice calibration was made with unheated primary air.

MIXING REGION TESTS

The initial test using the apparatus was primarily a check on serviceability and accuracy of instrumentation, the configuration being that of isothermal mixing without baffles. A limited number of velocity surveys of the mixing region showed the results to be in excellent agreement with that found by other investigators (Ref. 4 and 20) so it was concluded that the designed apparatus would be satisfactory for the present experiments.

The next two runs (heated primary but no baffles, and heated primary with wing baffles at one inch, data for which is not included in this report) consisted of temperature and velocity surveys across the mixing region at eight different points along the test section. The temperature and velocity profiles normal to the flow were adequate for comparison of results, but it was felt that more information regarding behavior of centerline flow values would be required to satisfactorily depict the relative effectiveness of the baffles to be used. Hence, as time did not permit the desirable expediency of increasing the number of complete flow traverses, it was decided to make only four traverses normal to the flow (one at the beginning of the mixing region, one that would be near the presumed potential core, and two downstream of the core), and to increase to twenty the number of centerline investigation points.

Although it would have made for more uniformity to conduct all experimental runs in a single day, the number of test

configurations made it impossible. Thus the final data, as reported herein, was obtained during three separate running periods: the no baffles, and the three wing baffle (at three different locations in the test section) configurations were first tested; next the three runs using the screen-plus-wing baffles, and lastly, the three screen baffle runs were made. Static pressure values for the wing baffle and no-baffle configurations were rechecked the day following the actual runs because a more accurate inclined manometer for reading static pressures was substituted. Agreement with the previous static pressure values was within the accuracy of the instruments used.

Before starting the test runs, the engine was warmed up, then the acetylene and spark were turned on with the primary air at the mass flow rate to be used for the test. After combustion was initiated and the spark turned off, the acetylene low pressure valve was adjusted until the reference thermocouple in the primary line, 35 inches upstream of the primary exit, reached a steady value that experience showed would produce a temperature of about 525 to 550 degrees F. at the end of the primary pipe. This upstream reference temperature was continuously read and recorded during the tests. A pressure reading of 5 to 6 psi. at the low pressure acetylene valve was found necessary to maintain temperature. Some attempts were made to meter the acetylene through a flow-rator, but the flow was much too small to be read with available

equipment. By weighing the acetylene tank before and after a run it was found that, roughly, the mass flow rate of acetylene was only .000115 lbs./sec. as compared to the average mass flow rate of primary air of 0.046 lb./sec.

In order to facilitate adjustment of the primary and secondary air flows, a series of curves (for various upstream orifice temperatures) of mass rate of air flow versus the product of pressure drop (in inches of water) across the particular orifice, times the upstream static pressure at the orifice (in inches of mercury) were plotted. Included on the same plots were another series of curves (for various temperatures of the primary or secondary flows at the beginning of the test region) of mass flow rate versus velocity at the beginning of the test section. A sample of these curves, for standard atmospheric pressure, are included in the Appendix as Figs. 19 and 20.

Fig. 21, also in the Appendix, is an example of the curves used to convert dynamic pressure q, in inches of water, to flow velocity for various temperatures.

Maintaining the desired flow rates was not difficult because of the relatively low values used. Although it would have been much more desirable to run all the tests at higher flow rates than those used, in order to have higher dynamic pressures in the test region for better accuracy in measurements (six to seven inches of water was the highest dynamic pressure recorded), it was not

possible because of the limitation on the primary air supply. Higher mass flow rates would have resulted in inadequate primary flow long before a particular run could be completed, with the resulting necessity of burner shutdown and subsequent difficult readjustment to the exact flow and heat values prevailing during the completed part of the run. As a result, the accuracy of the static pressure values, and of the smaller dynamic pressure values, is questionable.

All test runs were made with flow rates, temperatures, and initial velocities as nearly the same as possible, but some variations were unavoidable. However, in view of the dimensionless character of the final results obtained, and considering that the variations in flow parameters were not excessive, it is felt that qualitative comparison of the results is justified.

DISCUSSION OF RESULTS

GENERAL

Locations in the mixing region are defined by the dimensionless coordinates of X/D for positive distance downstream from the primary pipe exit, and Y/D for distances normal to the flow direction, from the zero value at the center of the primary pipe. Thus, the station at the boundary of the primary pipe at the beginning of the mixing region is X/D = 0, and Y/D = 0.5.

The dynamic pressure readings, with the simultaneous temperature values at the various points in the mixing region, were converted to velocity values in ft./sec. Values for primary undisturbed flow velocities for the various runs were chosen as the values obtained at X/D = 0 and Y/D = 0. These velocities were higher by 4.7 percent with heat, but no baffles, and by as much as 9 percent with screen-plus-wing baffles, than the primary velocities as computed from orifice measurements. The discrepancies were due, of course, to the profile of dynamic pressures and temperatures existing in the stream at X/D = 0. The profiles of temperature and velocity for the no-baffle configuration are presented as Fig. 3. That the discrepancies between the predicted and actual centerline velocities were not larger than they were, is probably due to the fact that the primary flow pipe contained two right angle elbows in the line between the heater box and primary exit, which produced

some turbulence, with resultant smoothing out of temperatures and velocities. The temperature gradient across the wall of the primary pipe, where the secondary air was surrounding it, probably accounts for much of the velocity and temperature variations that did exist at X/D = 0. Also, it is probable that the baffles in the flow introduced velocity variations upstream toward the beginning of the mixing region.

It is felt that choosing the lesser primary velocity (as predicted from flow rates) rather than the centerline value would not have resulted in as fair a comparison of the various baffled configurations. Only centerline values of velocity and temperature, obtained at the six-Volt center wire position, were measured, except at the four X/D stations of 0, 8, 12, and 20. At these stations complete traverses were made across the flow, readings being taken every 0.2 inch, plus a reading at X/D = 0.5.

NO BAFFLE CONFIGURATION

The no-baffle configuration was tested primarily to provide a reference for the baffled runs. Hence, the various curves obtained are redrawn on the various baffled configuration graphs. The data, as recorded and computed, is presented as a sample data sheet, Table II (Appendix).

The results of the no-baffle run, however, are interesting in the light of conclusions drawn by other investigators. To

compare shapes of velocity and temperature profiles normal to flow direction, Forrestal and Shapiro (Ref. 4), studying isothermal velocity and mass mixing, fully normalized the velocity profiles by making plots of the dimensionless ratios of $\frac{u-u_s}{u_c-u_s}$ against r/r_m, and found that these curves remained essentially unchanged at any X/D station beyond the potential core. They further found that the curves closely resemble a cosine curve defined by $\frac{u-u_s}{u_c-u_s} = \frac{1}{2}(1+\cos\frac{\pi}{2}\frac{r}{r_m})$. Even with heated primary air, it can be seen from Fig. 4a that the cosine curve is a good comparison with the normalized velocity profiles plotted for X/D = 12 and 20. The divergence of the experimental points from the theoretical at the greater values of r/r_m may be due to the limited accuracy of measurements of the low dynamic pressures with resultant difficulty in choosing the correct r_m value.

Similar normalized temperature profiles were also made at X/D = 12 and 20, as shown in Fig. 4b. Agreement with the cosine curve is good, only slight divergence resulting at the greater r/r_m values. Ruegg and Klug (Ref. 11) found that their temperature profiles showed greater divergence from the cosine curve, the further downstream the profile was made, and approached a distribution predicted by Tollmein. The curves shown herein also show a greater divergence for the profile at X/D = 20 than at 12.

It is interesting to note that the values of r_m, obtained for the velocity and temperature profiles at 12 and 20, also verify

the "accepted" conclusions from other investigators that temperature diffuses more rapidly than velocity. Thus, r_m (velocity) is 0.5 and r_m (temperature) is 0.6 at X/D = 13, and, at X/D = 20, the values are 0.7 and 0.91 for velocity and temperature, respectively.

Axial mixing, in accordance with accepted literature, is compared by using the dimensionless quantities $\frac{u_c-u_s}{u_p-u_s}$ or $\frac{T_c-T_s}{T_p-T_s}$ with the view that a jet in a general stream would mix and eventually approach the properties of the stream. Thus, a value of zero for this parameter would indicate 100 percent mixing. Forrestal and Shapiro, for the case of isothermal velocity mixing, found this ratio to have a value of unity up to the end of the potential core, indicating no change in centerline velocity, and then a decrease in the value of the ratio in inverse proportion to axial distance downstream of the potential core; i.e.,

$$\frac{u_c-u_s}{u_p-u_s} = \frac{L}{X/D} \quad \text{for } X/D > 1$$

They further concluded that the X/D value for the length L of the potential core can be approximately expressed as $L = 4 + 12\lambda$, where λ is the ratio of secondary to primary velocity. For a velocity ratio of 0.407, based on centerline value of primary velocity for the no-baffle configuration, the equation would give L = 8.9. The experimental value, as determined from Fig. 5, extrapolating the curve as a straight line back to the zero $\frac{u_c-u_s}{u_p-u_s}$ value, gives an X/D at the end of the potential core of

about 7.2, a difference of 19 percent. Although neither theory nor experimental evidence dictates that the relation between L and λ should hold with non-isothermal jets, it was decided to check if the difference between the two values for L could have been due to the high centerline primary velocity used in the computation. Recalculations of the values of $\frac{u_c-u_s}{u_p-u_s}$, based on the average primary velocity as determined from the known primary mass flow, were made, the velocity ratio then being 0.45. The formula then gives a value of 9.4 for L. The experimental value was found to be 7.6, although the curvature of the plot (not included herein) was somewhat decreased in the potential core region. The difference between the two L values is again 19 percent. Hence, it may be inferred that, based on the single non-baffled run investigated, and comparing with isothermal jet studies, the effect of the heated primary air is to improve the velocity mixing in an axial direction. This is not in accordance with the conclusions of Ruegg and Klug (Ref. 11) who state that the effect of compressibility is to retard mixing.

The plot of the temperature parameter, $\frac{T_c-T_s}{T_p-T_s}$, versus X/D, as shown in Fig. 6, does not show a well defined potential core of temperature, but rather a gentle curvature between X/D = 4 and 10. However, straightline extrapolation back to the zero value of $\frac{T_c-T_s}{T_p-T_s}$, indicates an X/D of 7.0 for the end of the potential core. Beyond the core, the equation of the variation becomes

$$\left(\frac{T_c-T_s}{T_p-T_s}\right)^{.745} = \frac{L}{X/D} \quad \text{for} \quad L = 7$$

Thus, the temperature function decreases with X/D increase at a rate faster than that predicted by Forestall and Shapiro for the isothermal velocity function, where the exponent of the corresponding velocity ratio was unity. It should be noted also that the value of 7, indicated herein for the temperature potential core, is greater than the value of 5.5 which was found by Ruegg and Klug to exist as a constant value for three of their test runs at various velocity ratios.

STATIC PRESSURES, GENERAL

Static gage pressures, in inches of water, as initially plotted for all test configurations, produced a wave shaped pattern of about 0.25 in. H_2O maximum variation from a mean value. Subsequent investigation proved the pattern to be the result of small variations in test section length as a particular run progressed. The variation in the section length was caused by the necessity of periodically removing the 12 inch sliding panel at the extreme downstream position and placing it at the beginning of the test section, as the four inch plate, with its probe and static pressure tap, was moved downstream.

In order to remove the wave effect, it was necessary to find the effect on static pressures due to changing duct length. Hence, a static pressure survey of the mixing region was made with only the secondary air flowing, at a mass rate corresponding to that

used during the test runs. Measurements of static pressure at a single X/D station, as the duct length was varied, gave the required corrections. It was found that the corrections required varied with the range of duct length changes; varying duct length from 72 to 60 inches, reduced the static pressure 0.276 inches of water, or an average of 0.023 in. H_2O per inch change of duct length. Varying the length from 62 to 50 inches gave a correction of 0.0085 in. H_2O per inch change in duct length, and changing the length from 50 to 38 inches, produced a change of 0.007 in. H_2O per inch change of duct length.

As the range of duct length changes required during the tests was in the 72 inch to 60 inch range, a value of 0.026 in. H_2O per inch change in duct length, from a basic length of 72 inches, was used to correct the test values of static pressure. This value, slightly greater than the 0.023 value determined experimentally, was found by trial and error to be the best average to remove the wave effect from the actual test runs. The increased value used is reasonable in that the corrections required were proven experimentally to be larger for greater overall lengths of duct length changes.

Figs. 7, 8, and 9 are plots of the corrected static pressures, in inches of water, versus X/D positions, for the baffles located at 1, 4, and 7 inches respectively. The pressures for the no-baffle configuration is reproduced on each graph for comparison purposes.

That a decrease in static pressure at some point in the duct should occur, with a decrease in duct length, is reasonable. With earlier expansion at the duct exit, for the shorter duct lengths, there is a slight velocity increase. The corrections that would be required to the dynamic pressure values, due to changing duct length, are small however, as can be shown by equating mass flows for two different duct lengths. See Sample Calculations. Hence, dynamic pressures and velocities were not corrected for the changing duct length effect.

An estimated friction drop, due to the duct walls themselves, was obtained from the experimental run with secondary air only, so that any pressure losses would be due to friction and not from mixing. The average drop was estimated to be .005 to .010 inches of water per inch duct length, at test values of secondary mass flow. Applying this drop to the overall pressure drop for the no-baffle configuration, gives a pressure drop, due to mixing action only, of about 0.1 to 0.2 inch H_2O. That this is a reasonable value can be verified by the conservation of momentum equation, using average values of primary, secondary, and mixed dynamic pressures from the no-baffle configuration test run. The pressure drop, so calculated in the Sample Calculation section, is found to be 0.21 inches of water.

It was originally intended to correct the static pressures for the friction effects so that the pressure drops would represent

losses due to mixing action (and baffles) only. However, in view of the limited accuracy of the friction drop, and the resulting decrease in the pressure drop for the no-baffled configuration, it was decided to record and use pressures in terms of losses due to mixing and friction. The doubtful accuracy of the static pressures because of the small magnitudes, would not justify using the extremely small pressure differences, due to mixing action only, for the no-baffle configuration, in any computations. As explained later in this report, the pressure differences between two X/D stations were used as a divisor in mixing effectiveness calculations.

BAFFLED CONFIGURATIONS, GENERAL

The effects of placing baffles in the mixing region were reflected in the static pressure values, and in the lateral and axial velocity and temperature distributions. All the runs were made with approximately the same secondary and primary mass flows, (about 1.57 and 0.046 lb. of air per second, respectively), and the resultant dynamic pressures at X/D = 0 were comparable. The variations that did exist can be attributed to the higher static pressures at the zero position when the baffles were in the duct: a rise in static pressure upstream of a baffle would have to be accompanied by a corresponding decrease in the average dynamic pressure, providing equal mass flows produce equivalent total pressure levels.

It is not believed that flow reversal occurred at any point in the test section where readings were taken, because the dynamic pressure values never approached zero. A thin metal rod, with wool tufts attached, was probed into the mixing region at various points, before and aft of the baffles, to allow the tufts to align themselves with the streamlines. Flow disturbances, while obviously existent from the behavior of the fluctuating tufts, were not producing any noticeable flow reversals. Rotation of the pitot tube, to a position not aligned with the duct axis showed a greater dynamic pressure, in several instances, when the wing-baffles were being tested. This increase was probably due to tip vortices caused by the wings. All dynamic pressures recorded however, were for the pitot axis parallel with the duct axis, i.e., pointing into the supposed flow direction.

BAFFLED CONFIGURATIONS--LATERAL VELOCITY DISTRIBUTION

Comparison of velocity distributions normal to the flow are not particularly informative because the velocity levels at a particular X/D station differed widely with the baffle configurations; for example, the screen-plus-wing baffle, located at X/D = 4, shows a centerline velocity of only 94 ft./sec. at X/D = 12, while the screen-baffle has 120 ft./sec., the wing-baffle 132 ft./sec., and the no-baffle configuration, 160 ft./sec., at the same X/D = 12 position. (See Fig. 10a) This is because the velocity mixing effect

prior to station X/D = 12 has been very pronounced, particularly for the screen configurations (with their large pressure drop). Thus, it is not possible to say which baffle arrangement would give the best lateral velocity mixing, given the same initial velocities at the same X/D station.

If normalizing the profiles, as previously described, provides a fair basis for comparison, then, from Fig. 11a, the wing baffle at X/D = 4 configuration can be considered to give the best mixing, because the steeper the curve, the faster is the approach to a mixed condition. Due to the velocity fluctuations in the screen-plus-wing baffle configuration, it was not feasible to normalize that profile.

In an effort to better compare the transverse mixing, Fig. 12 is presented. A normalized velocity profile for one each of the three baffles tested are shown. The values of the center-line velocities and secondary velocities were approximately 120 and 90 ft./sec. respectively, for each of the tests at the X/D stations noted. The profiles are at an X/D of 12 for the screen-baffle at four inches, at 12 for the wing-baffles at one inch, and at eight for the screen-plus-wing baffles at four inches. The wing configuration appears to give a more uniform and initially faster approach to the mixed condition, while the two other baffle types approach the fully mixed condition at a smaller value of r/r_m.

Thus, velocity gradients for the screen and screen-plus-wing baffles would be greater.

For information, the following table gives the maximum velocity at the indicated X/D stations, expressed as a multiplier of the minimum velocity at the same X/D, for the various runs:

	X/D = 8			X/D = 12		
Baffle	At 1"	At 4"	At 7"	At 1"	At 4"	At 7"
Wings	1.77	1.98	2.26	1.33	1.41	1.7
Wings and Screens	1.28	1.33	1.21	1.14	1.18	1.13
Screens	1.4	1.49	1.66	1.39	1.33	1.24

BAFFLED CONFIGURATIONS--LATERAL TEMPERATURE DISTRIBUTION

Comparison of temperature profiles are also difficult because of the temperature levels at a particular X/D. Fig. 10, (b), shows the actual profiles at X/D = 12, with the three baffles located at X/D = 4. Comparison with the no-baffle curve, also shown, indicates that, of the baffled runs, only the wing-baffle produced a uniform mixing tendency. The screen configuration, due to poorer axial temperature mixing upstream of X/D = 12, shows a centerline temperature almost 140° F. higher than the no-baffle configuration, while the screen-plus-wing baffle run produced a temperature, at Y/D = 0.4, higher than its centerline value. This

same result was noticed in the two other screen-plus-wing baffle runs, but the reason for the variation is not clear. If it were due to the tip vortices from the wings, one would expect to find a similar temperature increase away from the axis when the wings were tested alone. However, this effect was found to a minor degree in only one run using the wing-baffles alone. This was at X/D stations of 8 and 12, with the baffles located at X/D = 7. If the higher temperature had been found at a lesser value of Y/D, the discrepancy could have been attributed to mal-positioning of the probe, but it is not very likely that an error of 0.3 to 0.4 of an inch in Y/D positioning of the probe could have been consistently made for the three screen-plus-wing runs.

Normalized temperature profiles for the wing-baffles and screen-baffles at 4 inches, are shown in Fig. 11b. Good agreement with the cosine curve is noted at the smaller r/r_m values. At the larger values, the curve for the wing-baffles approaches the mixed condition faster than the cosine curve, while the screen configuration shows a slower approach to the zero temperature difference ratio.

It appears that the effect of the screens is to equalize the pressures across the test section, while having little effect on the temperatures. Thus, the velocities, being proportional to the square root of the dynamic pressures and to the first power of absolute temperatures, are quickly equalized.

BAFFLED CONFIGURATIONS--AXIAL VELOCITY DISTRIBUTION

Figs. 5, 13, and 14 are log-log plots of the velocity parameter $\frac{u_c-u_s}{u_p-u_s}$ versus X/D position, for the various runs, with the baffles located at X/D = 1, 4, and 7 respectively. The no-baffle curve is shown on each graph for comparison. In all cases, the baffles improve velocity mixing as compared to the no-baffle run. The location of the end of the potential core was greatly influenced by the position of the baffles, especially when the screen or screen-plus-wings were used. It is noted that the curves begin to diverge from the near unity value of $\frac{u_c-u_s}{u_p-u_s}$ about one inch upstream of the baffle location for either screen-type baffle, and about one inch downstream of the baffle location for the wing-baffle configuration. In other words, the wings are not as effective in promoting velocity mixing if the large pressure losses inherent with the screen arrangements are not considered. The screen-plus-wing baffle runs approach the mixed condition more quickly than any of the other runs. The curves are much more regular for the wing-baffles, and beyond the potential core the rate of decrease of $\frac{u_c-u_s}{u_p-u_s}$, with increase in X/D, is very nearly the same as for the no-baffle configuration. The wing-baffles seem to shorten the potential core and then permit normal mixing to occur.

Correlation of the pressure drops with the percent mixing attained, will be discussed after the axial temperature distribution is considered.

BAFFLED RUNS--AXIAL TEMPERATURE DISTRIBUTION

Figs. 6, 15, and 16 are log-log plots of $\frac{T_c-T_s}{T_p-T_s}$ versus X/D for the three baffle types located at X/D = 1, 4, and 7 respectively. Again the curve for the no-baffle run is included for comparison.

Here, the only baffle at all effective in bringing the streams to a common temperature is the wing configuration at all three locations used. With the baffles at X/D = 7, the mixing action is only slightly better than the no-baffle arrangement, and located at X/D = 1 and 4, the effect of the wing-baffles appears nearly equal, but considerably better than the no-baffle run.

An interesting trend is noticed when the screen-plus-wing baffle curves are compared with the screen alone curves. In all three baffle locations, the screen-plus-wing arrangement shows an initial attempt to give good temperature mixing, probably due to the action of the wings. However, at about six inches after the baffle position in each case, the beneficial action of the wings appears to die out, and the decrease of the $\frac{T_c-T_s}{T_p-T_s}$ parameter is practically stopped until the curves meet the screen-baffle curve at about an X/D of 30. This may be regarded as further evidence of the beneficial action of the wings in promoting temperature mixing, and of the poor action of the screens in even allowing normal temperature mixing to proceed.

No reasonable explanation has been found for the apparent effect of the screens, in actually retarding axial temperature mixing, when compared to the no-baffle configuration.

MIXING EFFECTIVENESS

In order to qualitatively correlate the mixing attained at a particular X/D station, at the expense of pressure drop resulting for the various configurations, a "mixing effectiveness" parameter has been devised. This parameter may be defined as the ratio of the percent axial mixing attained, at a particular X/D station, to the static pressure drop at that X/D position. The mixing attained is based on centerline approach of the primary stream velocity or temperature to the secondary stream velocity or temperature; i.e., percent mixing attained $= \left(1 - \frac{u_c - u_s}{u_p - u_s}\right) 100$ or $\left(1 - \frac{T_c - T_s}{T_p - T_s}\right) 100$.

The pressure drops at a particular X/D station are taken as the difference between the corrected static pressure at X/D = 0 and the corrected static pressure at the particular X/D. Division by the primary air dynamic pressure value at X/D = 0, Y/D = 0, makes the pressure drops dimensionless and comparable. Figs. 7, 8, and 9 are plots of the static pressures corrected for changing duct length, as previously described, versus X/D position, for the baffles located at 1, 4, and 7 X/D stations respectively.

Table I is a tabulation of the percent centerline mixing as read from the faired curves of Figs. 5, 13, and 14 for velocity,

and from Figs. 6, 15, and 16 for temperature. The pressure drops recorded are the values read from the curves of Figs. 7, 8, and 9. The values of the "mixing effectiveness" parameter, as then computed and tabulated in the table, are shown in Fig. 17 for velocity and Fig. 18 for temperatures, for various X/D stations.

Due to the large pressure drops resulting from use of the screen configurations, these baffles produced very low values of the mixing parameter for both velocity and temperature mixing. Their values are not individually plotted, but are shown as a range of values on the graphs.

The no-baffle configuration naturally shows a relatively high value of mixing effectiveness, due to the low values of pressure drop.

The wing-baffles, located at X/D = 4, is the only baffle configuration that makes a better showing than the no-baffle run. The wing-baffle at X/D = 1 produced too high a static pressure at the zero position with resulting greater drop, and the wings at X/D = 7 position, while having pressure drops comparable to the wings at X/D = 4 position, was too slow in giving a good value for centerline mixing.

It is noted that, as far as velocity mixing is concerned, the wing-baffles, at X/D = 4, gives higher values of "mixing effectiveness" than any other configuration, including the no-baffle run, between the X/D positions of 8 and 13. As short duct

length with adequate mixing is desirable in practical mixing applications, it may be inferred that the wing-baffles can prove advantageous in reducing mixing chamber length without producing excessive pressure losses.

Inspection of Fig. 18, the mixing effectiveness curve for temperature mixing, shows that none of the baffled runs are as effective as the no-baffle arrangement except between X/D values of 8 and 9. In this narrow range, the wing-baffle, located at X/D = 4, has the higher mixing effectiveness value because of the shorter potential core of temperature. Beyond station 9, the pressure drop associated with the baffle, allows the no-baffle run to display the highest mixing effectiveness values.

Inspection of the static pressure curves for the wing-baffle configurations shows that the large pressure drop immediately downstream of the baffle is partially recovered within two inches aft of the baffle location, and that the pressure rise ahead of the baffle is at its lowest value about one inch ahead of the baffle. Thus, if the wing-baffles were located at an X/D of about 2, the potential core would be shortened from the value at the X/D = 4 baffle location, to a value near to that attained with the baffles at X/D = 1. The mixing attained at the lower value of X/D would be correspondingly increased, and the difference between initial static pressure and pressure at X/D stations of 3 or 4 and beyond, would not be excessive. Hence, wing-baffles located at an X/D of

about 2 would probably show considerably better mixing effectiveness values at the smaller, more important X/D stations, than the no-baffle configuration.

Obviously, the individual values of mixing effectiveness as reported herein, are of no quantitative value. The fact that the magnitudes of static pressures as measured were so small, and of questionable accuracy, places considerable doubt on even the relative magnitudes of corrected pressure differences. Division by the difference of two already small numbers, as required in the mixing effectiveness calculations, is not conducive to accurate and really comparable results. A much higher total pressure level for running the tests would be required to produce true, reproducible values for pressure losses. Such higher pressure levels were not attainable with the available equipment, as explained in the Procedure section.

In practical applications, a more realistic "mixing effectiveness" parameter should give more weight to mixing attained at small X/D values, and less weight to the pressure drops resulting, depending on the losses that can be tolerated in order to attain short mixing chambers. It is believed that the wing type baffle configuration, however, has been proven to be worthy of further study and investigation.

CONCLUSIONS AND RECOMMENDATIONS

Temperature and velocity surveys of the mixing region formed by a cold air stream, surrounding and concentric with a hot gas stream, under steady flow conditions, have been conducted. Three different baffle arrangements, each tested independently at three positions in the mixing region, are compared with a non-baffled configuration as to temperature and velocity mixing effectiveness. The average velocity ratio of secondary stream (cold) to primary stream (hot), during the tests was about 0.4, at a Reynolds number of 57,000, based on the primary flow orifice diameter of one inch.

In terms of the approach of centerline velocity values to the velocity of the surrounding secondary stream, the screen baffles and the wing-plus-screen baffles, produced the best velocity mixing, if the resultant static pressure losses are ignored. In terms of a "mixing effectiveness" parameter, $\left[= (1 - \frac{u_c - u_s}{u_p - u_s}) 100 \right]$ which is defined as the ratio of the centerline mixing attained to a dimensionless pressure drop required, the stub wing baffles, located four inches from the beginning of the mixing region, is the only baffle arrangement to give a higher value of mixing effectiveness than the no-baffle configuration. These higher values occur at the smaller X/D values, the dimensionless distance from the beginning of the mixing region.

using stub wing "turbulence promoters" be made. Relocation of the baffles to an X/D of 2, variation of angle of attack of the wings from the ten degrees used, and variation in the span of the wings might well produce better mixing with a smaller pressure drop than was found in this investigation.

REFERENCES AND BIBLIOGRAPHY

1. F. W. Godsey, Jr. and L. A. Young, "Gas Turbines for Aircraft", McGraw-Hill Book Company, New York, 1949.

2. E. Kohler, "Notes on Steady Flow Combustion", Unpublished Notes for AE 411 Course, Internal Combustion Engines, U. S. Naval Postgraduate School, Annapolis, Md. 1951.

3. C. Ferrari, "Transport of Vorticity through Fluids in Turbulent Motion", L'Aerotecnia, Vol. 15, 1935. (Translated as N.A.C.A. T.M. 799.)

4. W. Forestall and A. H. Shapiro, "Momentum and Mass Transfer in Coaxial Gas Jets", Journal of Applied Mechanics, Vol. 17, No. 4, Dec. 1950.

5. W. Cleeves and L. M. K. Boelter, Chem. Eng. Prog., Vol. 43, p. 123, March 1947.

6. H. B. Squire, "Reconsideration of the Theory of Free Turbulence", Abstract in Philosophical Magazine, Vol. 39, pp. 1-20, Jan. 1948.

7. H. B. Squire and J. Trouncer, "Round Jets in a General Stream", A.R.C. (Gt. Brit.), Report 1974, Jan., 1944.

8. S. Corrsin and M. S. Uberoi, "Further Experiments in the Flow and Heat Transfer in a Heated Turbulent Air Jet", N.A.C.A. T.N. 1856, April, 1949.

9. S. Corrsin, "Investigation of Flow in Axially Symmetrical Heated Jet of Air", N.A.C.A. Wartime Report A.C.R. 3L23, Dec. 1943.

10. S. Corrsin and M. S. Uberoi, "Investigation of the Behavior of Parallel Two-Dimensional Air Jets", N.A.C.A. Wartime Report A.C.R. No. 4H24, Nov. 1944.

11. F. W. Ruegg and H. J. Klug, "Analytical and Experimental Studies with Idealized Gas Turbine Combustors", National Bureau of Standards Report 1B105, October, 1951.

12. R. L. Larson and others, "Effects of Turbulence Promoters in Refrigerant Evaporator Coils", Refrig. Eng., 57:1193-5, Dec. 1949.

13. L. G. Seigel, "Effect of Turbulence Promoters on Heat Transfer Coefficients for Water Flowing in Horizontal Tubes", Heating, Piping, and Air-Conditioning, Vol. 18, pp. 111-14, June, 1946.

14. Folsom and Ferguson, "Jet Mixing of Two Liquids", A.S.M.E. Vol. 71, pp. 73-77, 1949.

15. K. S. M. Davidson, "Use of Turbulence Producing Devices in Model Experiments", Marine Eng., 53-73, Dec. 1948.

16. "Cut Your Smoke by Increasing Turbulence", diags. Power, 91:407-8, June, 1947.

17. J. B. Verdin, "The Analytical Design of a Turbo-Jet Combustion Chamber", Master's Thesis, University of Minnesota, August, 1949.

18. "Jet Propulsion", Air Technical Service Command, 1946. (Restricted)

19. Flow Measurement, 1949, A.S.M.E. Power Test Code, 19.5; 4-1949.

20. C. Burton, "Preliminary Investigation of the Mixing of a Pulsating Air Jet in a Stead Secondary Airflow", Master's Thesis, University of Minnesota, August, 1951.

21. H. B. Nottage, "Turbulence-Fundamental Frontier in Air Distribution", Heating, Piping, and Air-Conditioning, Vol. 4, April, 1949, pp. 115-122.

22. Calhoun and King, "Heat Transfer and Pressure Drop in Empty, Baffled, and Packed Tubes", Ind. Eng. Chem., 1931, Vol. 23, pp. 916-923.

23. A. B. Binnie, "The Turbulent Spreading of a Water Jet", Engineering, Vol. 153, pp. 503-504, 1942.

24. C. B. Millikan, "Aerodynamics of the Airplane", John Wiley and Sons, Inc., New York, 1941.

25. O. W. Eshbach, "Handbook of Engineering Fundamentals", John Wiley and Sons, Inc., New York, 1936.

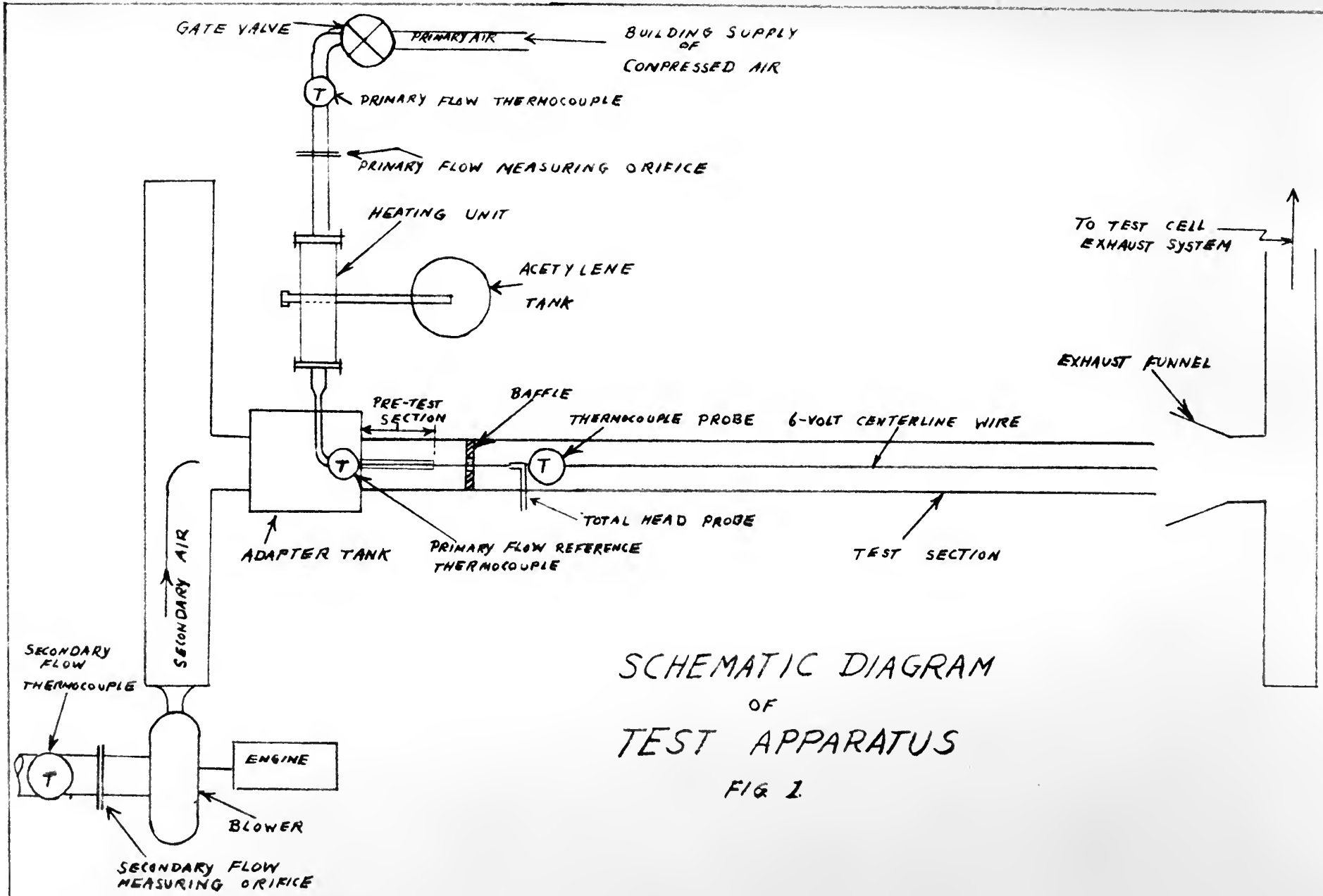

SCHEMATIC DIAGRAM OF TEST APPARATUS

FIG 1.

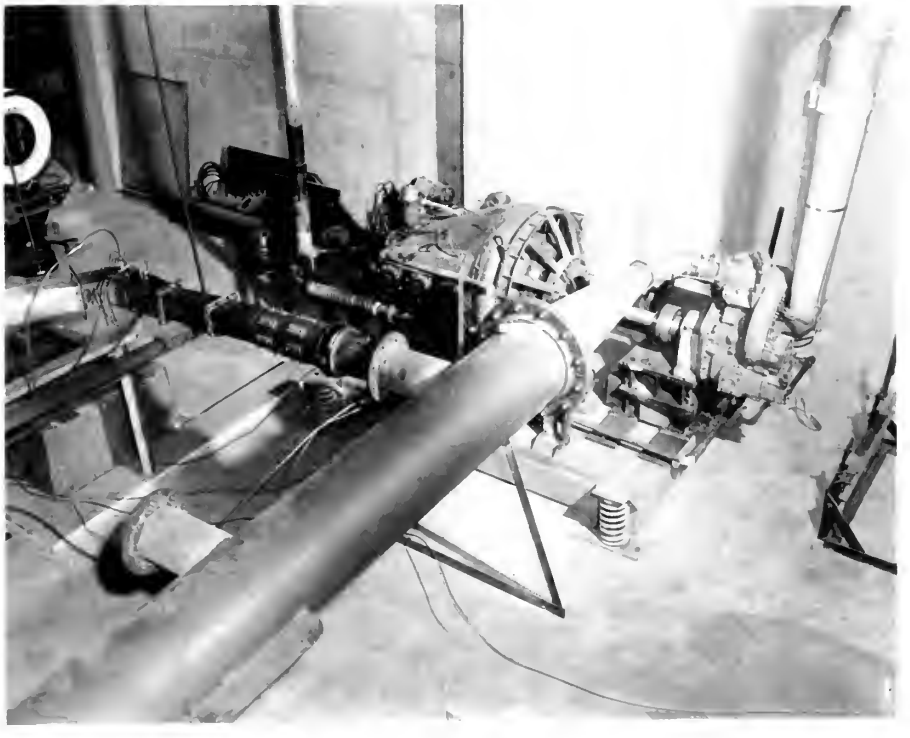

Fig. 2-a Engine, blower, and manifold

(The test set-up shown is not part of this experiment)

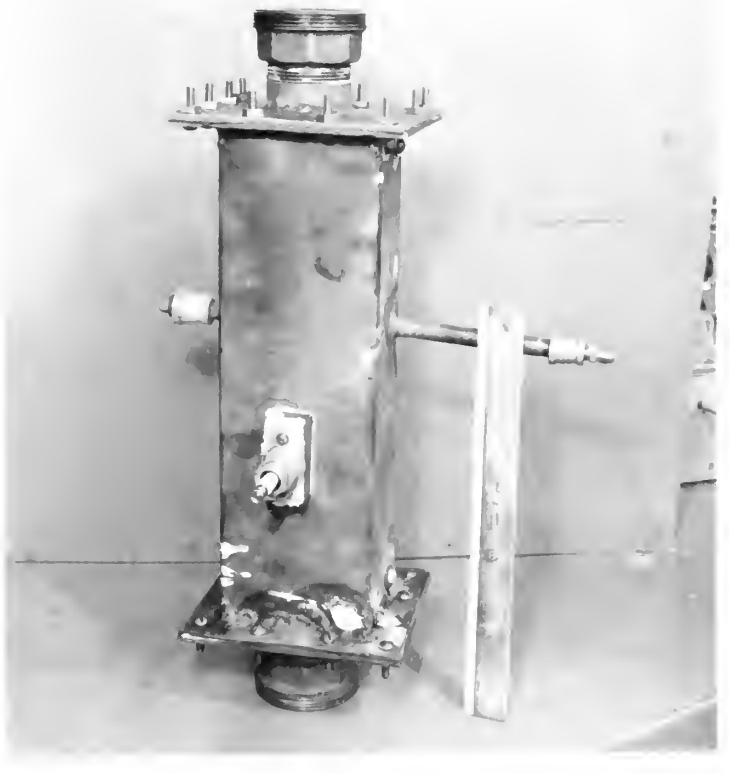

Fig. 2-b Heating Unit

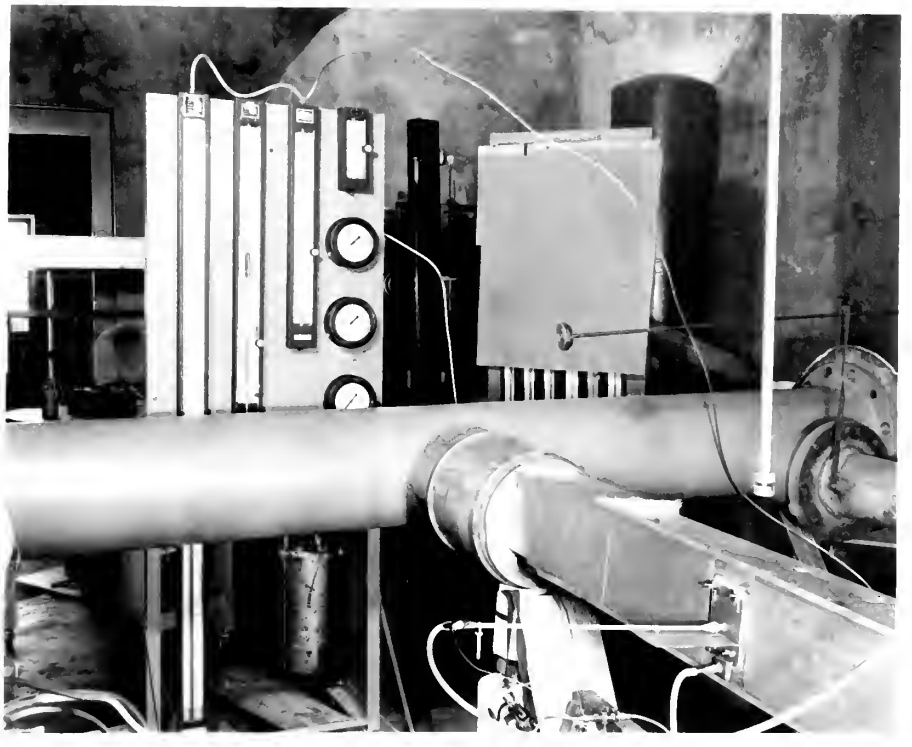

Fig. 2-c Test section and instrumentation

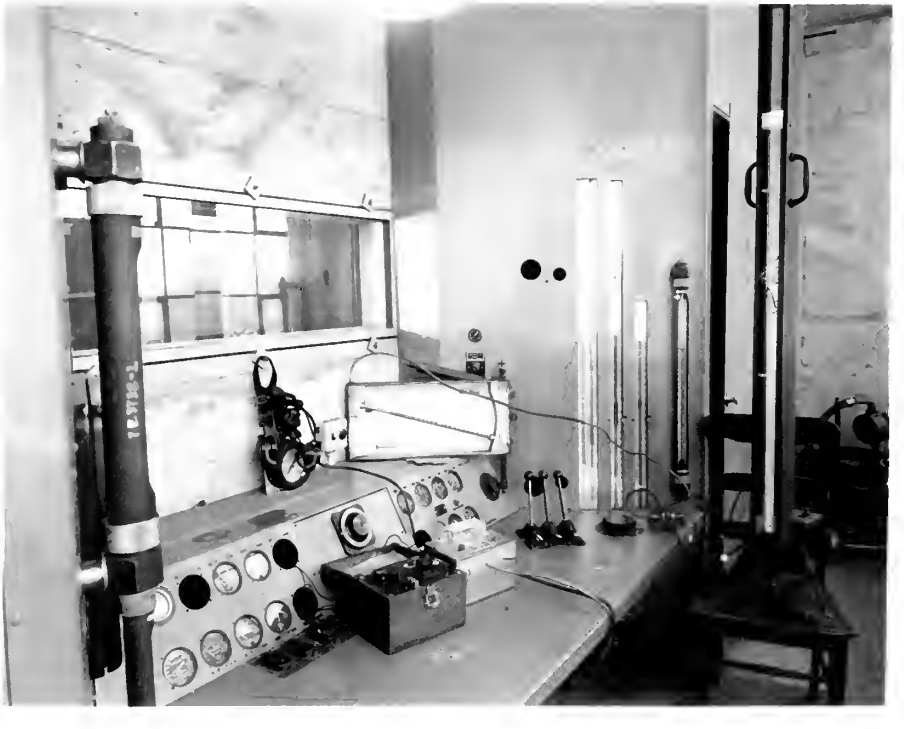

Fig. 2-d Control panel for engine operation

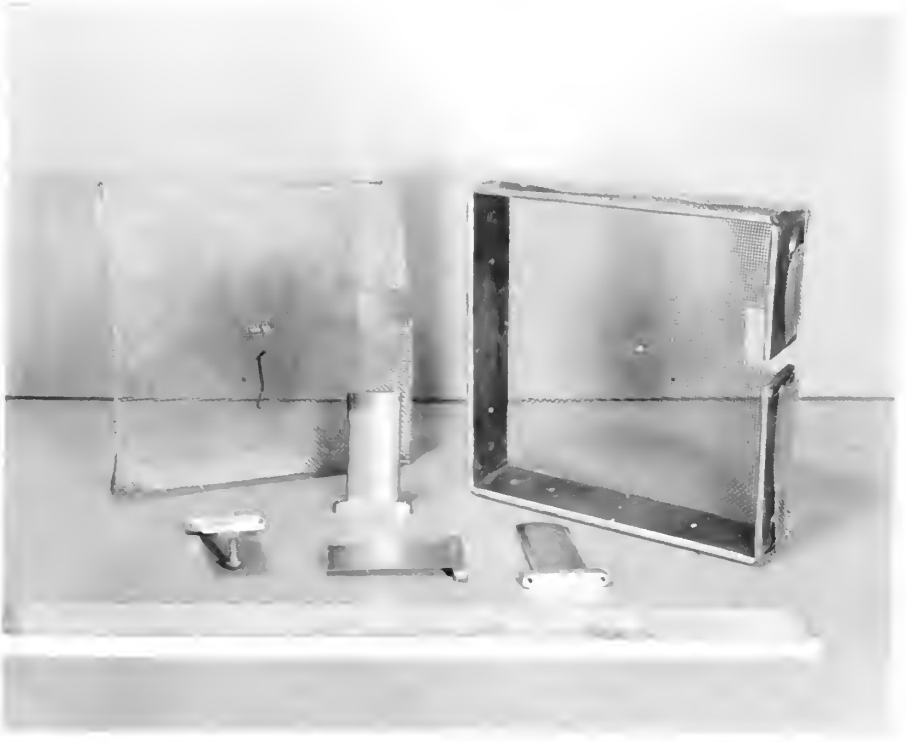

Fig. 2-e Component parts of the baffles

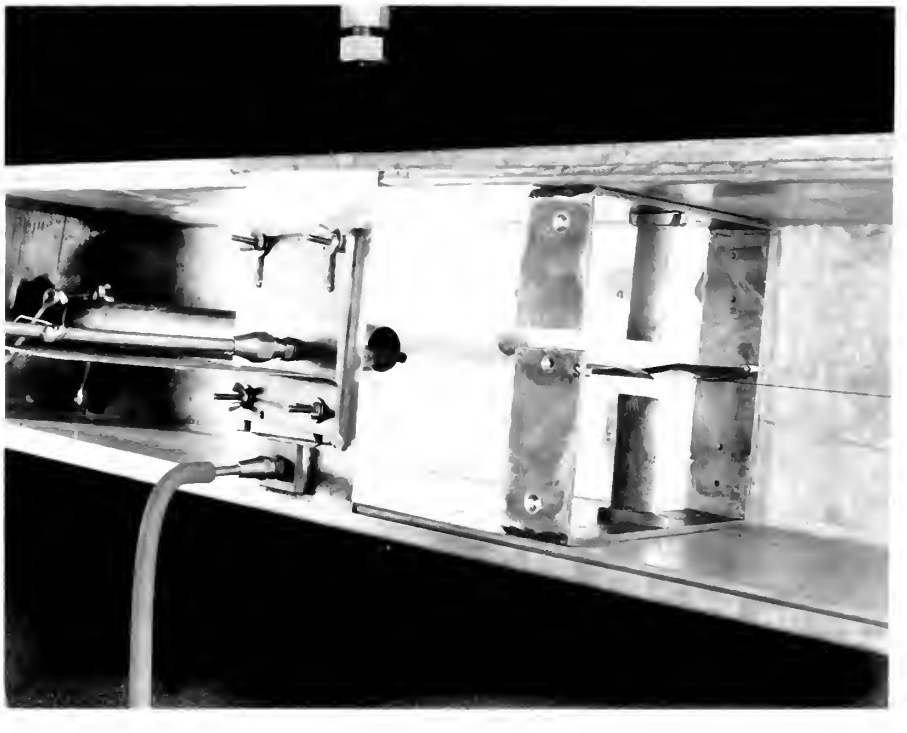

Fig. 2-f Wing baffles located in test section

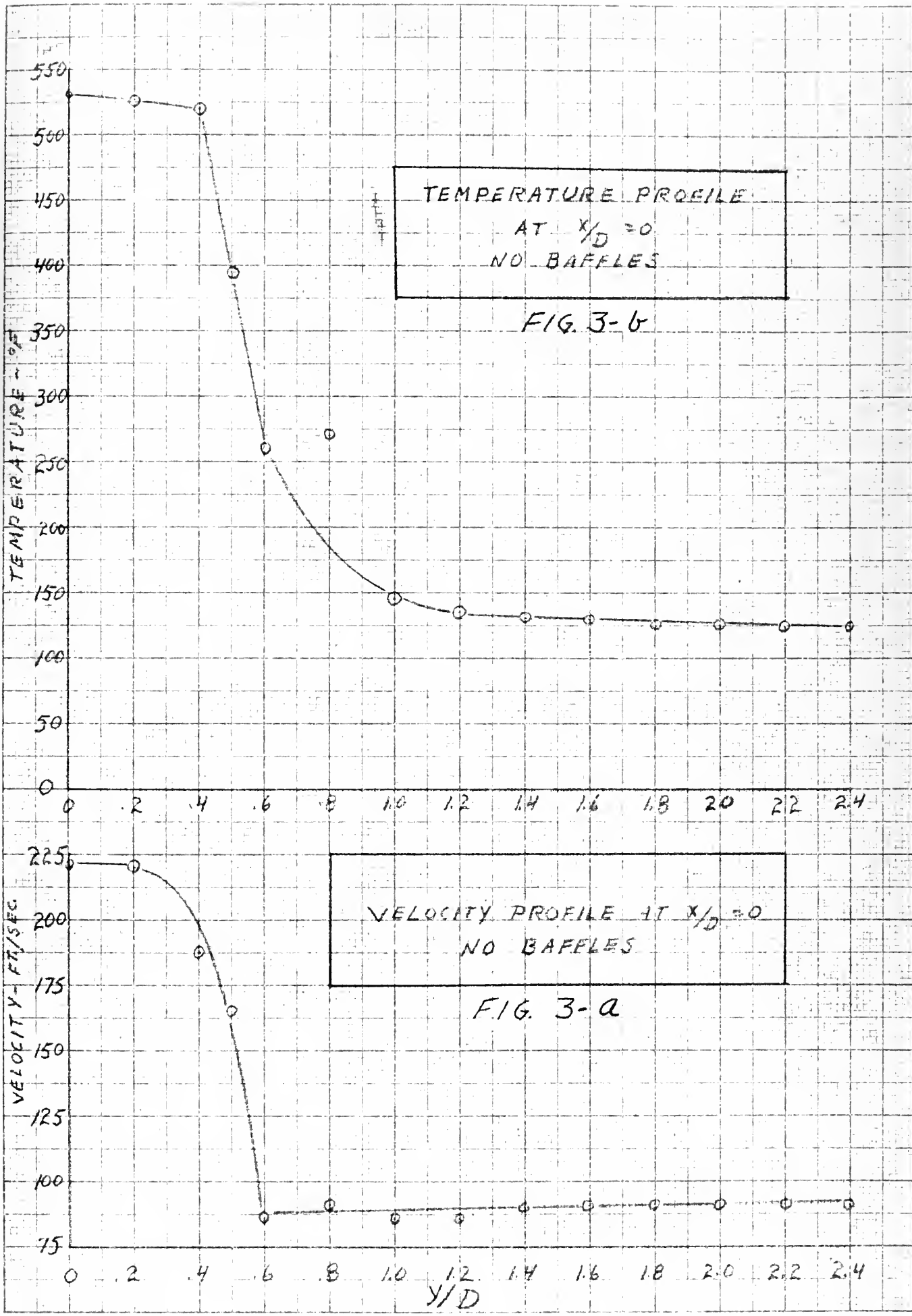
TEMPERATURE PROFILE
AT X/D = 0
NO BAFFLES
TEMPERATURE - °F
550
500
450
400
350
300
250
200
150
100
50
0
0 .2 .4 .6 .8 1.0 1.2 1.4 1.6 1.8 2.0 2.2 2.4

FIG. 3-b

VELOCITY PROFILE AT X/D = 0
NO BAFFLES
VELOCITY - FT/SEC.
225
200
175
150
125
100
75
0 .2 .4 .6 .8 1.0 1.2 1.4 1.6 1.8 2.0 2.2 2.4
Y/D

FIG. 3-a

NORMALIZED VELOCITY PROFILES NO BAFFLES

FIG. 4-a

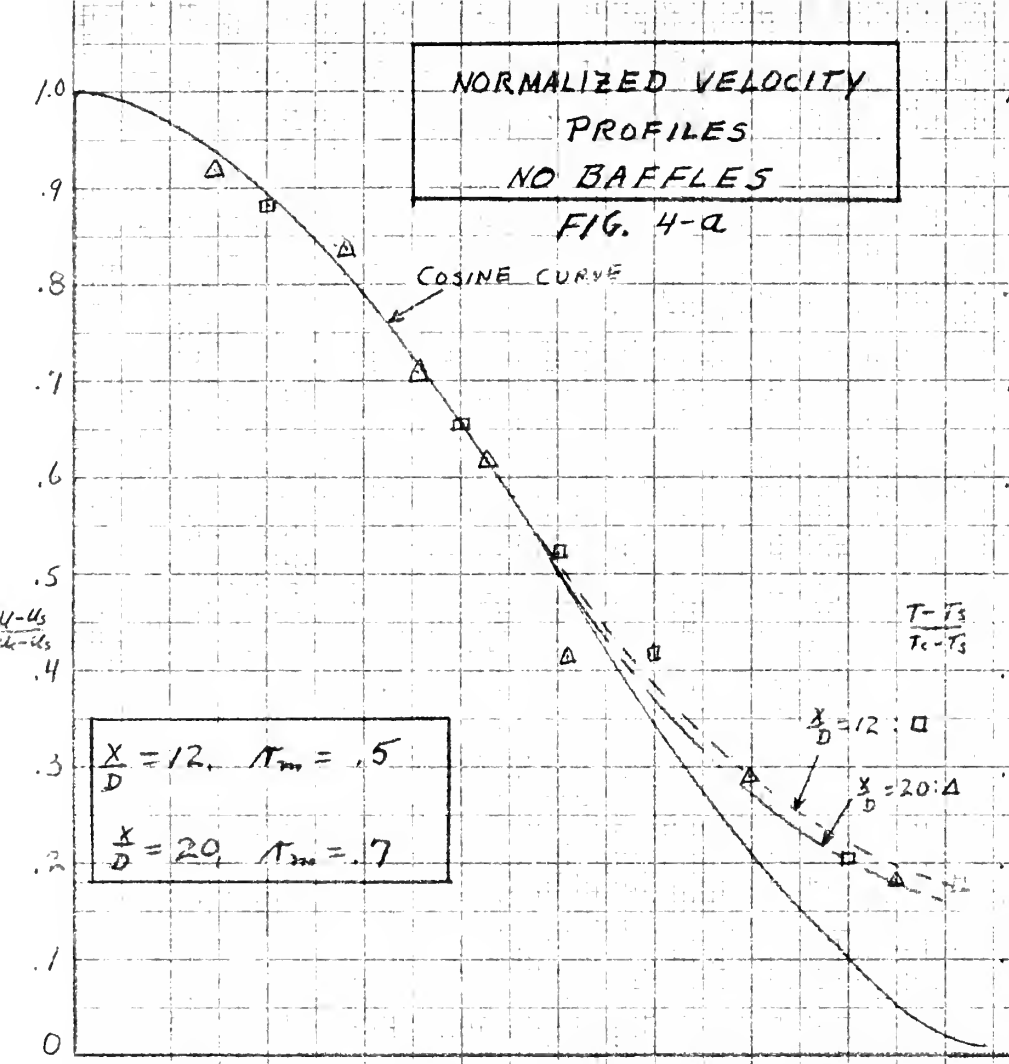

NORMALIZED TEMPERATURE PROFILES NO BAFFLES

FIG. 4-b

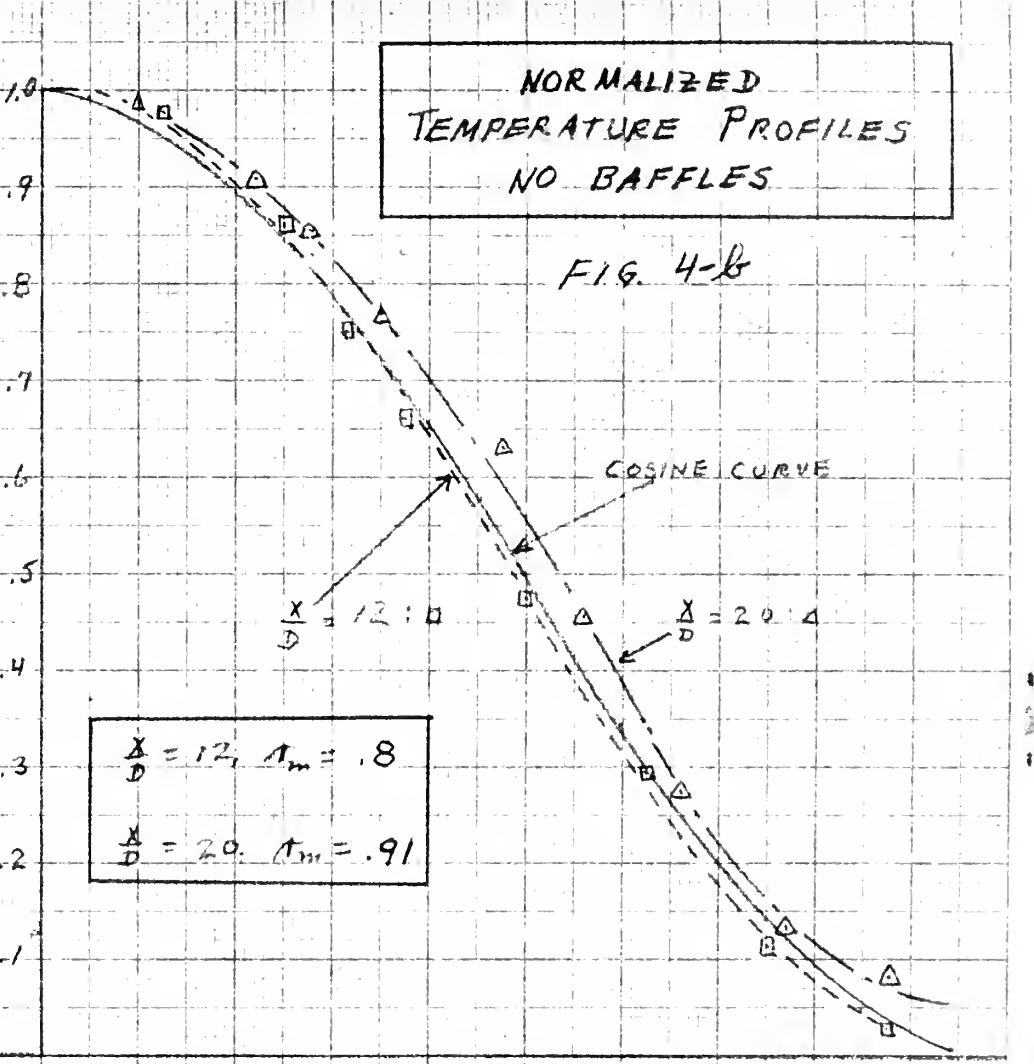

CENTERLINE VELOCITY DISTRIBUTION

BAFFLES AT $X/D = 1$

FIG. 5

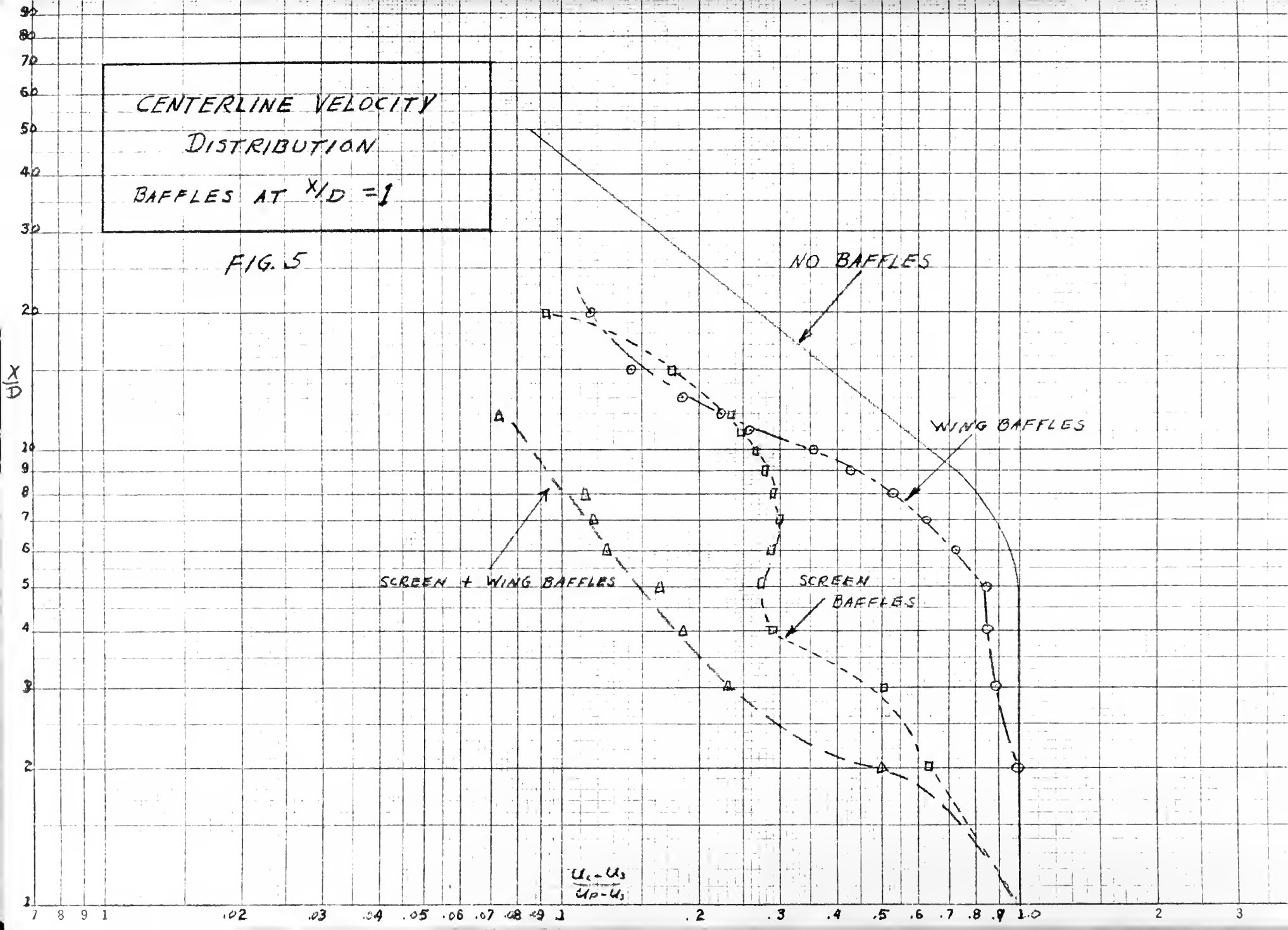

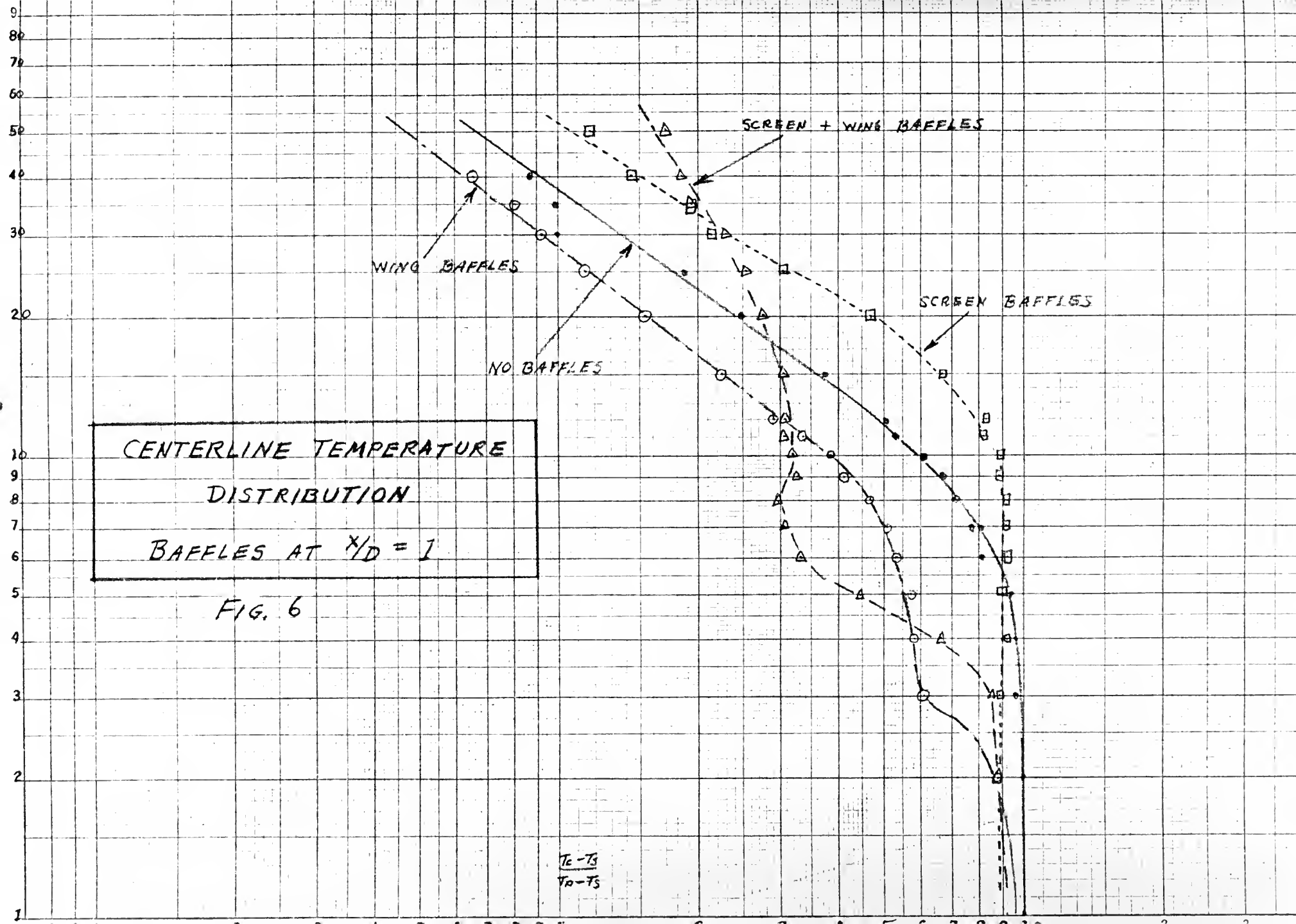

CENTERLINE TEMPERATURE DISTRIBUTION

BAFFLES AT $X/D = 1$

FIG. 6

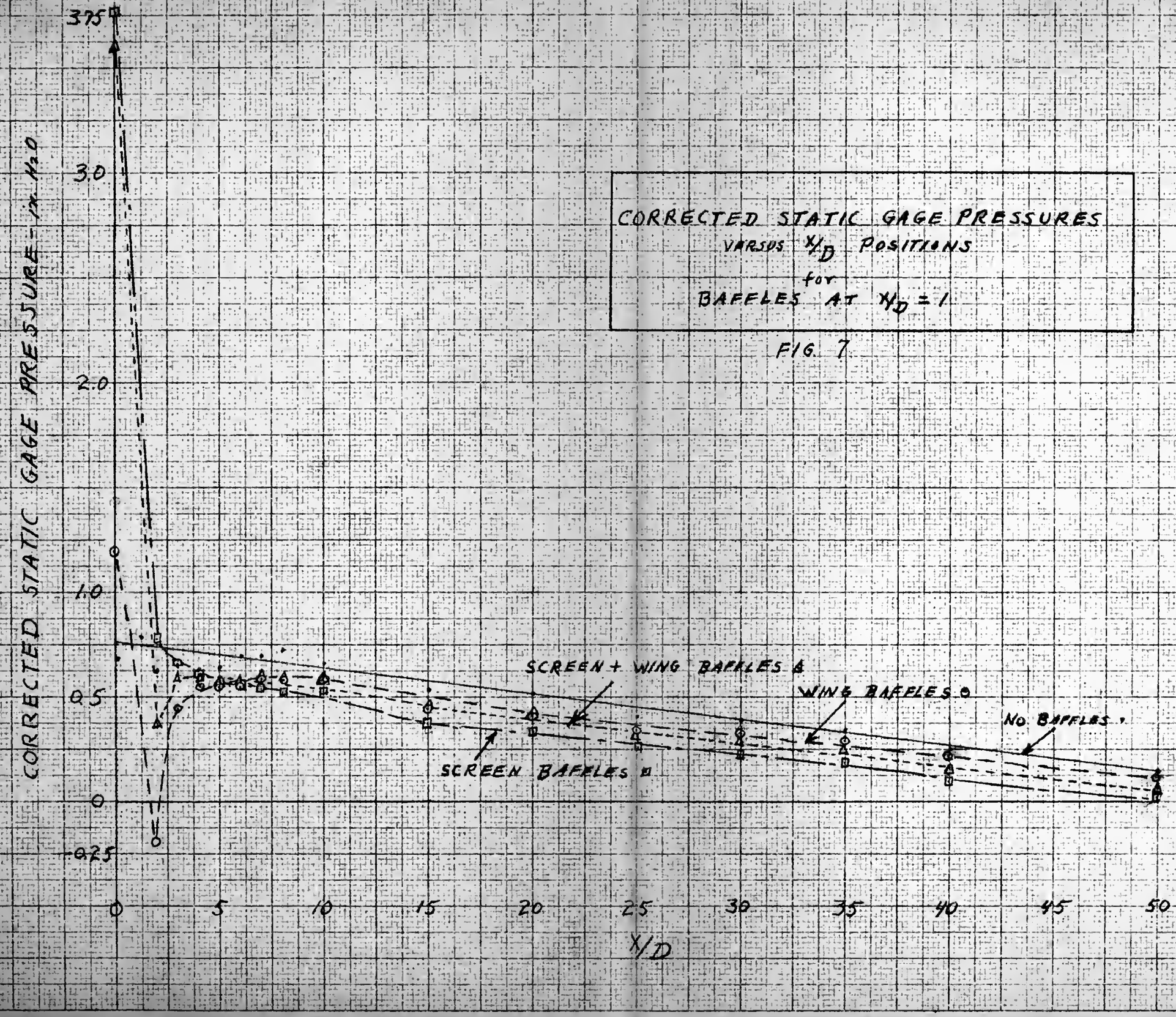

CORRECTED STATIC GAGE PRESSURES
VARSUS X/D POSITIONS
for
BAFFLES AT $X/D = 1$

FIG. 7

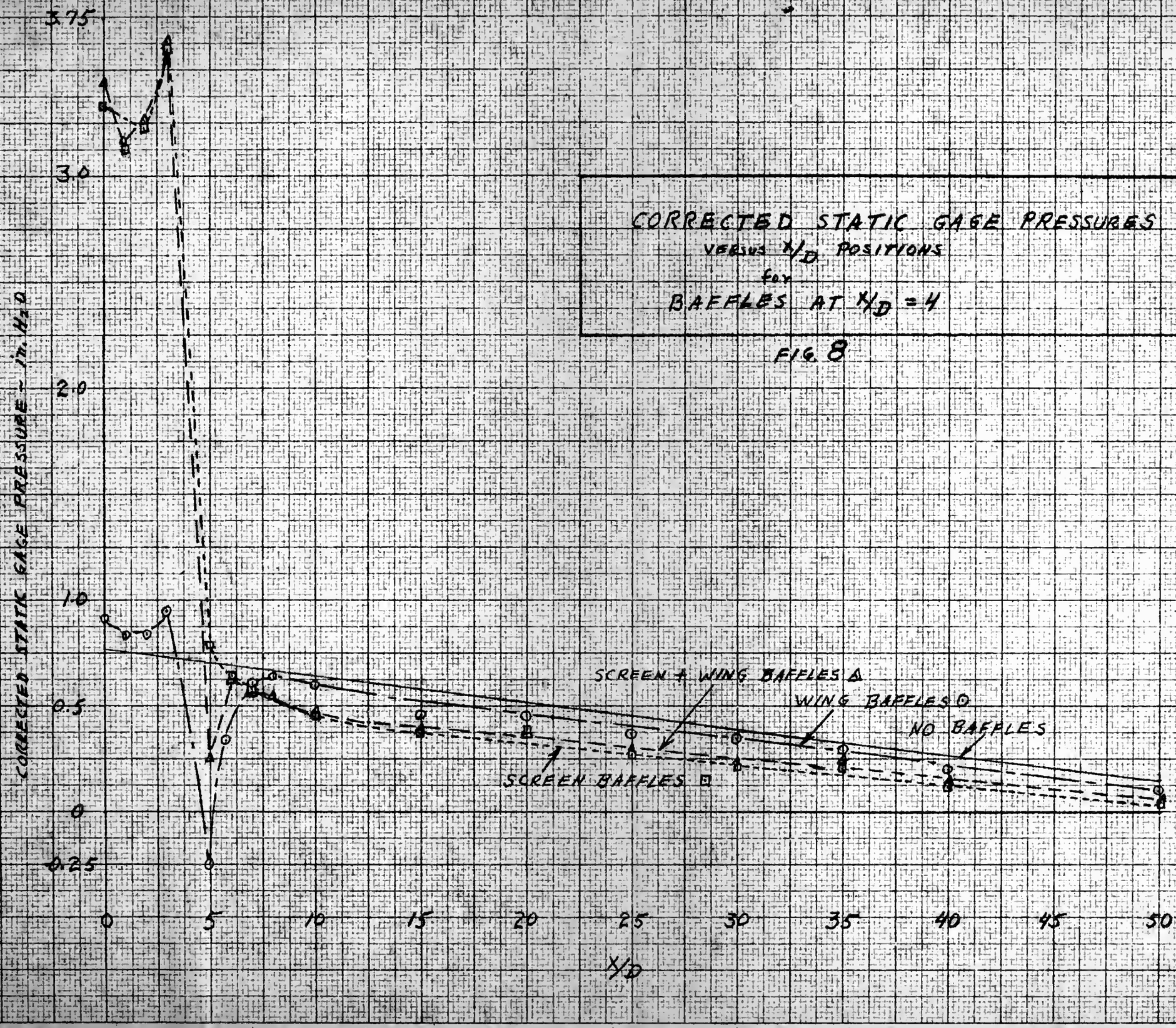

CORRECTED STATIC GAGE PRESSURES
versus X/D POSITIONS
for
BAFFLES AT $X/D = 4$

FIG 8

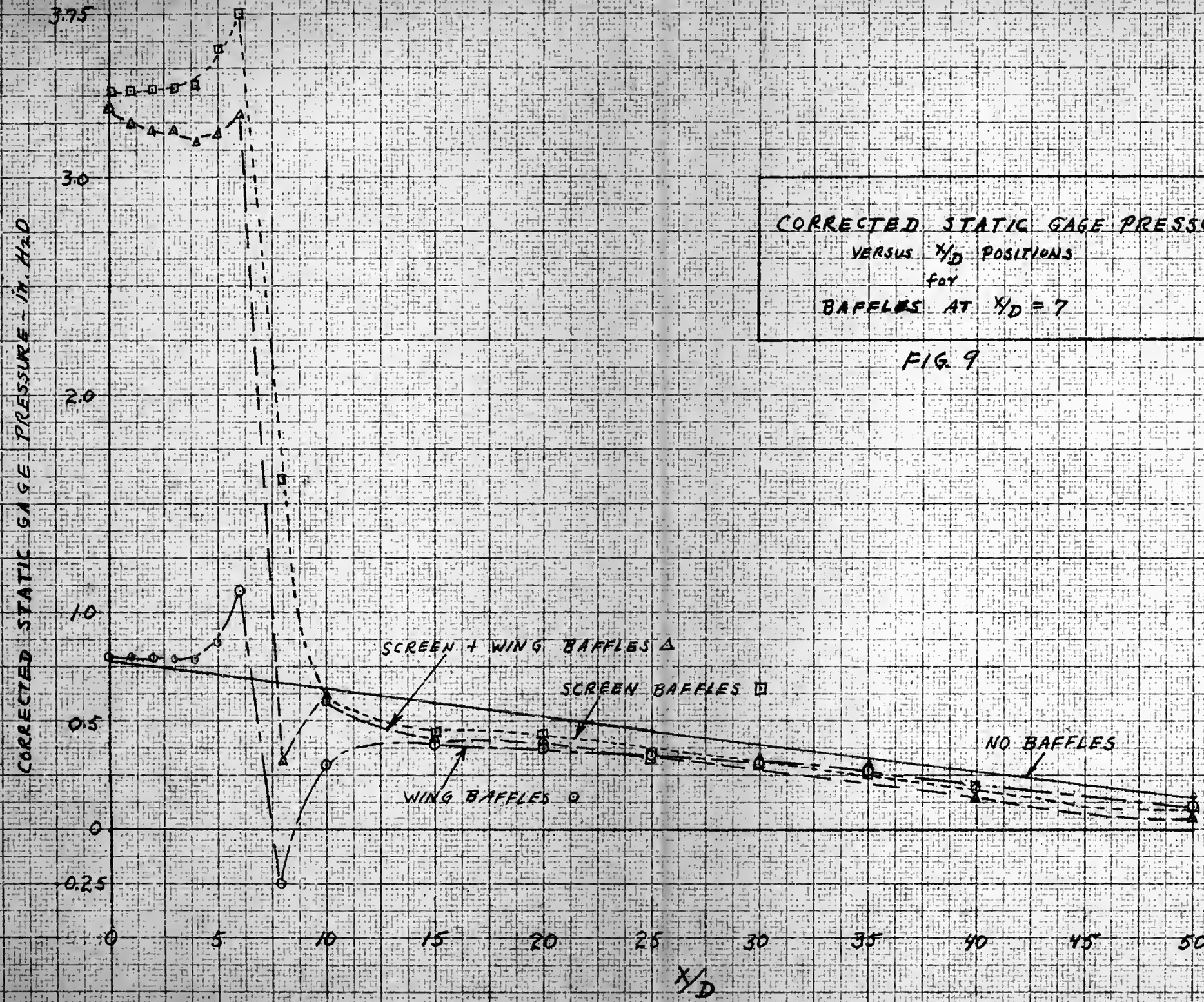

CORRECTED STATIC GAGE PRESSURES
VERSUS X/D POSITIONS
FOR
BAFFLES AT $X/D = 7$

FIG 9

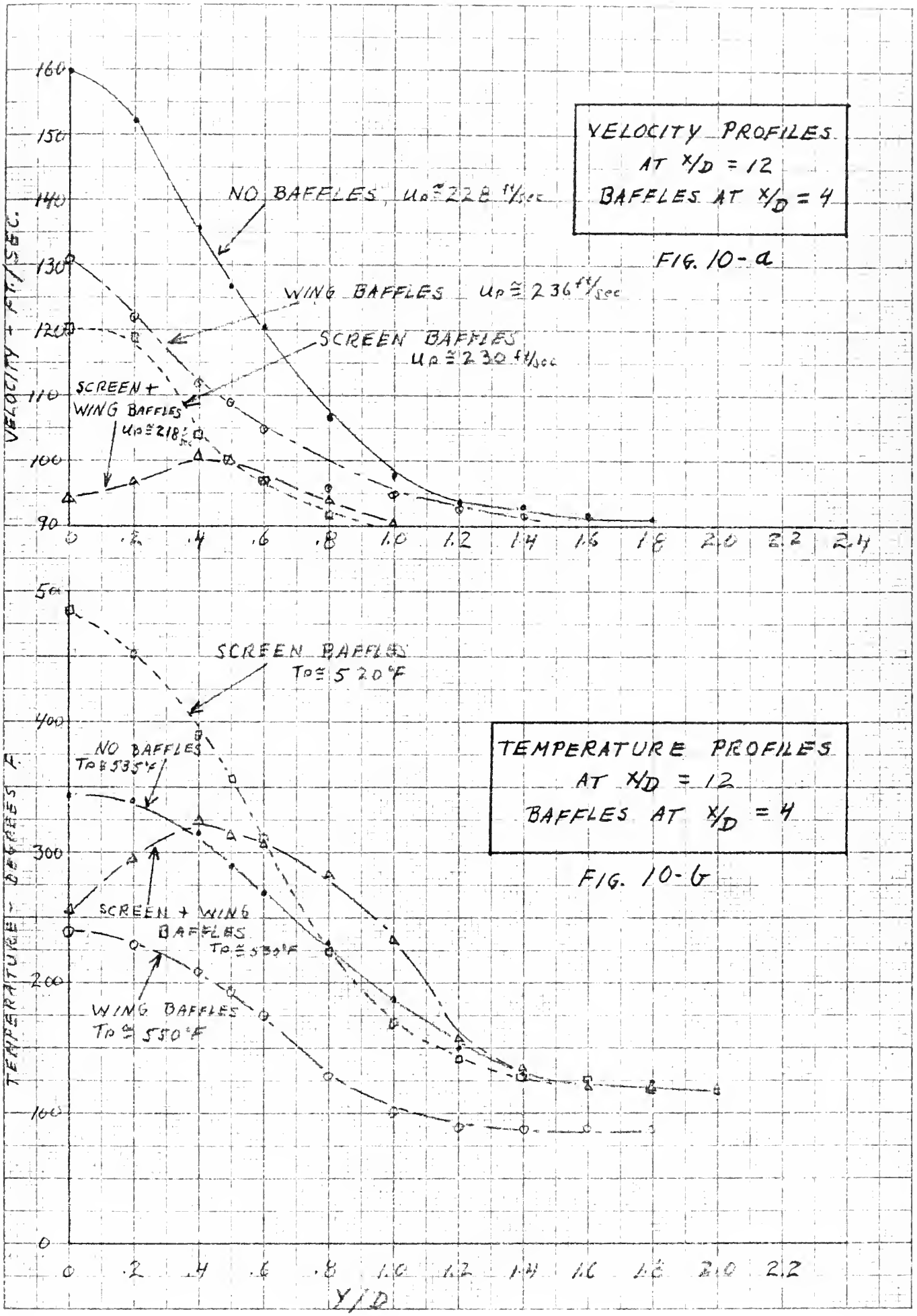
VELOCITY PROFILES
AT X/D = 12
BAFFLES AT X/D = 4
FIG. 10-a
NO BAFFLES, Uo ≅ 228 ft/sec
WING BAFFLES Uo ≅ 236 ft/sec
SCREEN BAFFLES
Uo ≅ 230 ft/sec
SCREEN + WING BAFFLES
Uo ≅ 218 ft/sec
VELOCITY - FT./SEC.
160
150
140
130
120
110
100
90
0
.2
.4
.6
.8
1.0
1.2
1.4
1.6
1.8
2.0
2.2
2.4
TEMPERATURE PROFILES
AT X/D = 12
BAFFLES AT X/D = 4
FIG. 10-b
SCREEN BAFFLES
To ≅ 520°F
NO BAFFLES
To ≅ 535°F
SCREEN + WING
BAFFLES
To ≅ 530°F
WING BAFFLES
To ≅ 550°F
TEMPERATURE - DEGREES F.
500
400
300
200
100
0
0
.2
.4
.6
.8
1.0
1.2
1.4
1.6
1.8
2.0
2.2
Y/D

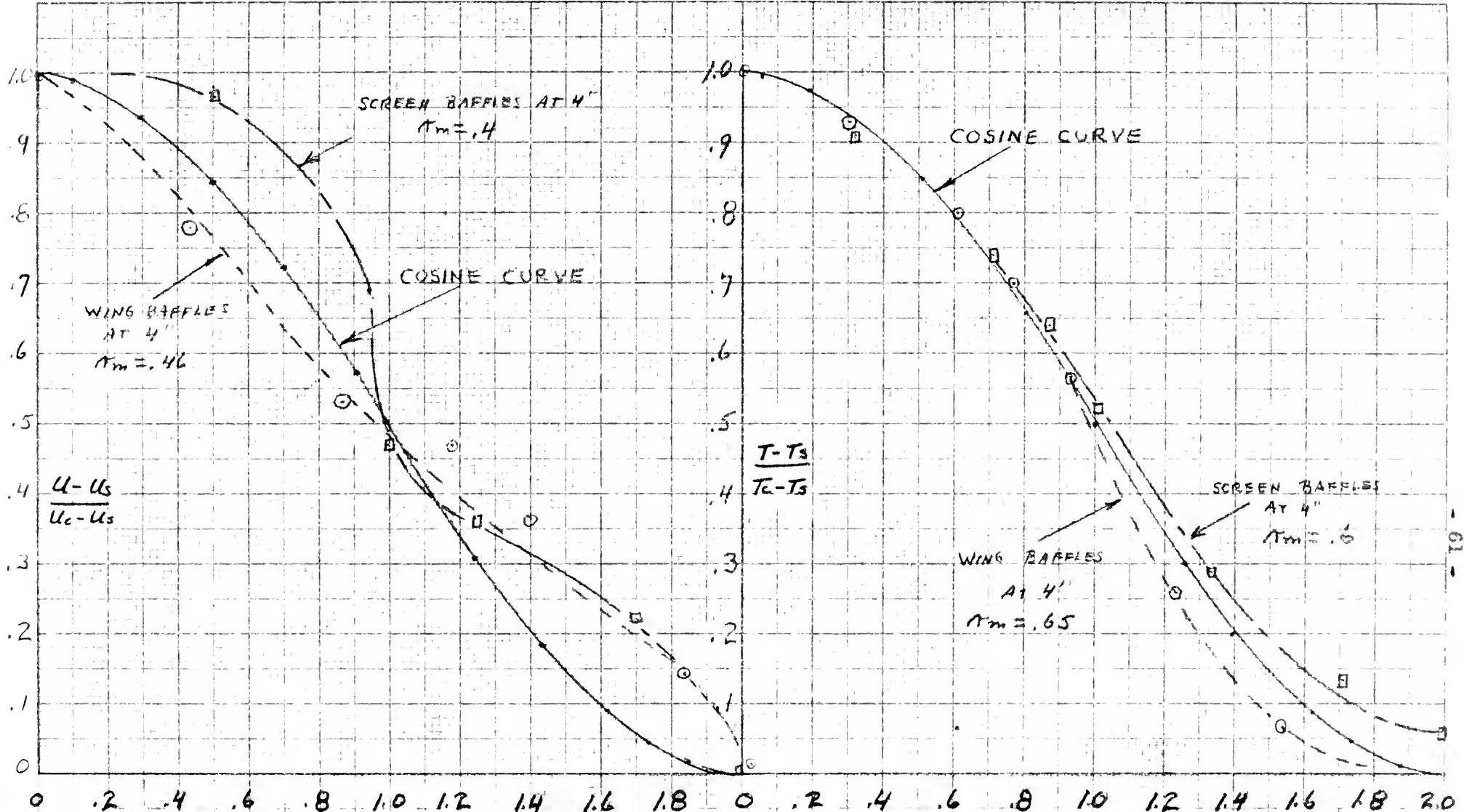

FIG 11-a

NORMALIZED VELOCITY DISTRIBUTION AT $x/D = 12$

FIG 11-b

NORMALIZED TEMPERATURE DISTRIBUTION AT $x/D = 12$

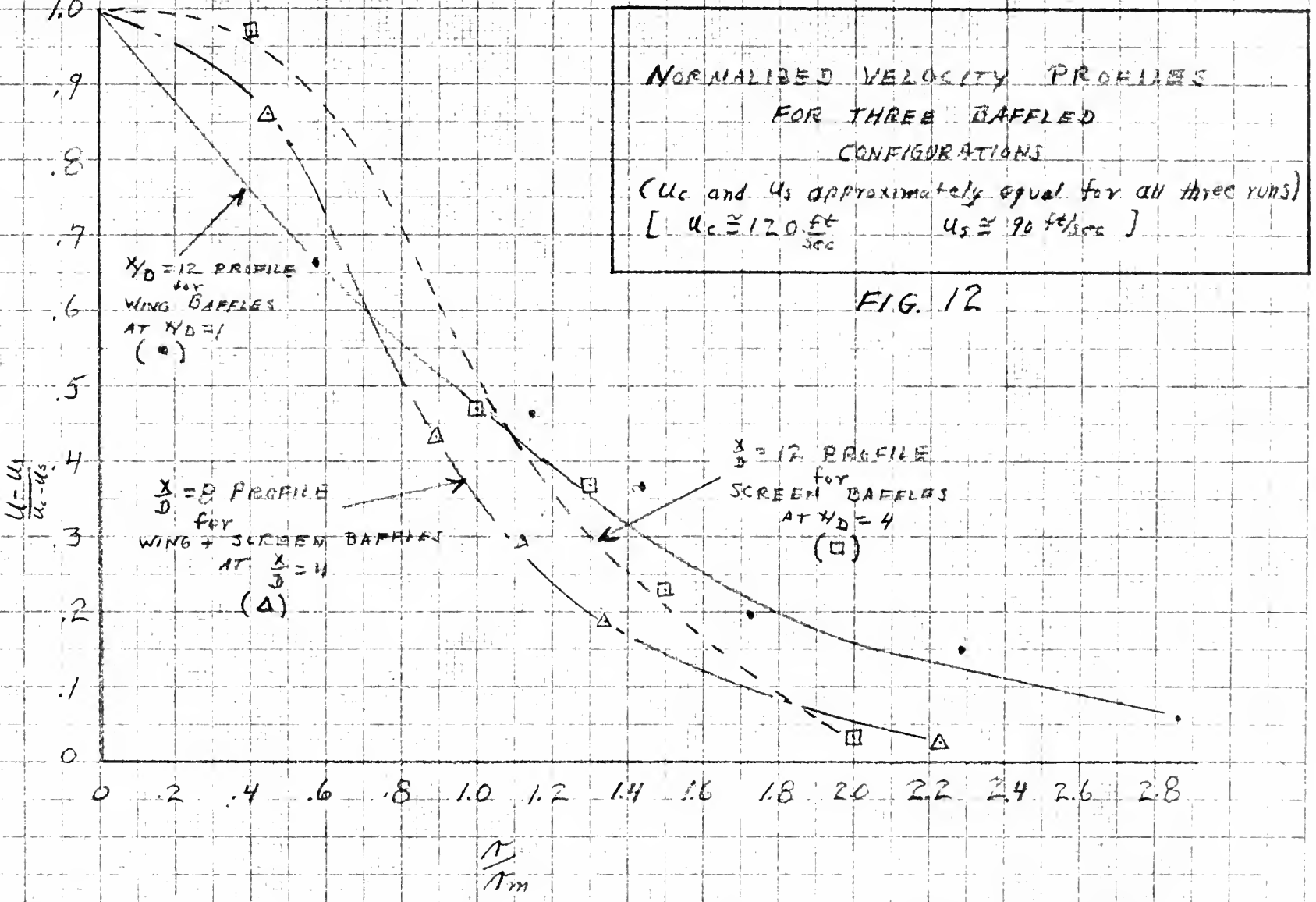
NORMALIZED VELOCITY PROFILES
FOR THREE BAFFLED
CONFIGURATIONS
(Uc and Us approximately equal for all three runs)
[Uc ≅ 120 ft/sec Us ≅ 90 ft/sec]
X/D = 12 PROFILE for WING BAFFLES AT X/D = 1 (•)
X/D = 8 PROFILE for WING + SCREEN BAFFLES AT X/D = 4 (△)
X/D = 12 PROFILE for SCREEN BAFFLES AT X/D = 4 (□)
(U − Us)/(Uc − Us)
r/rm
1.0
.9
.8
.7
.6
.5
.4
.3
.2
.1
0
0 .2 .4 .6 .8 1.0 1.2 1.4 1.6 1.8 2.0 2.2 2.4 2.6 2.8

FIG. 12

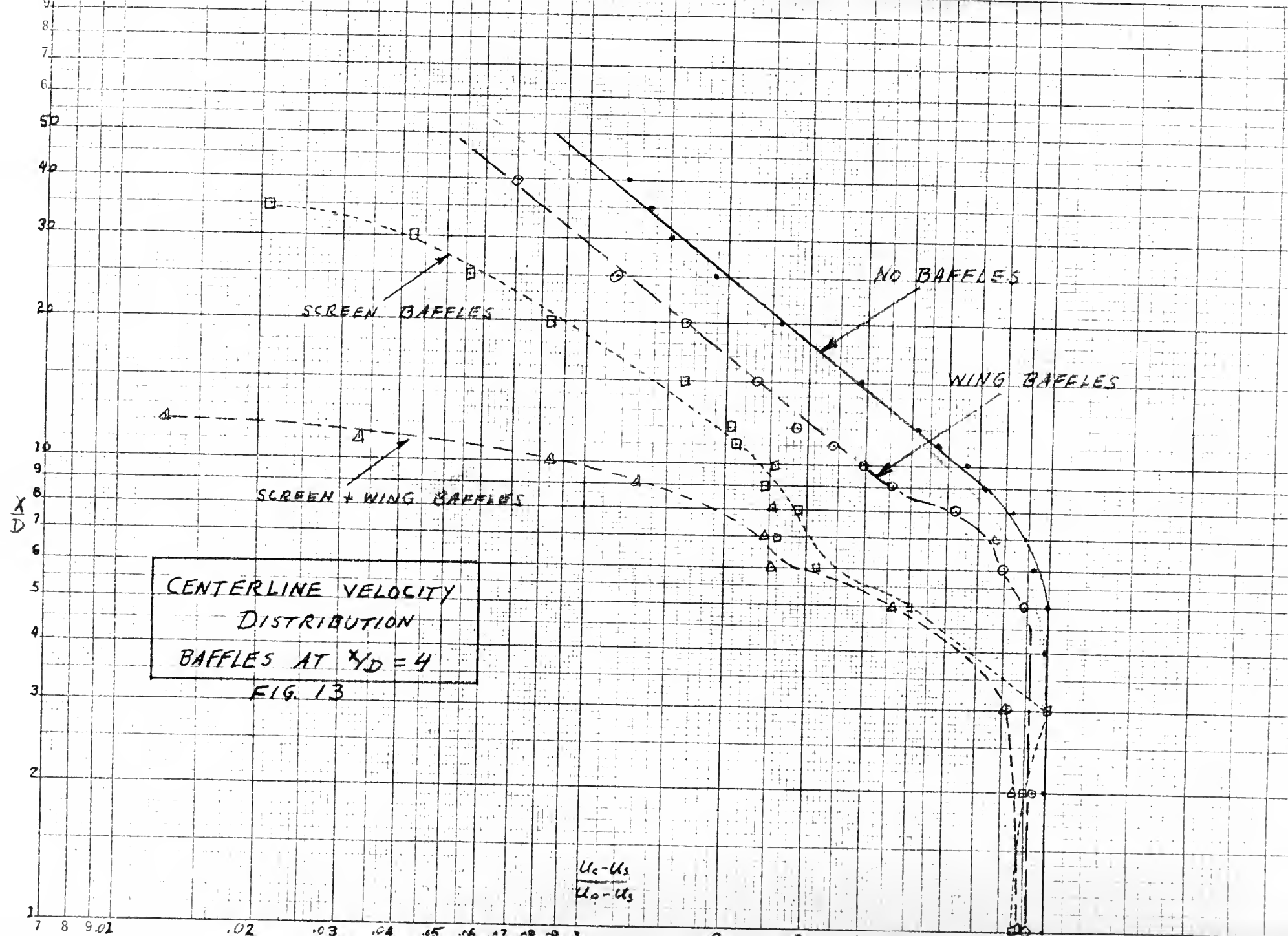

CENTERLINE VELOCITY DISTRIBUTION
BAFFLES AT $X/D = 4$
FIG. 13

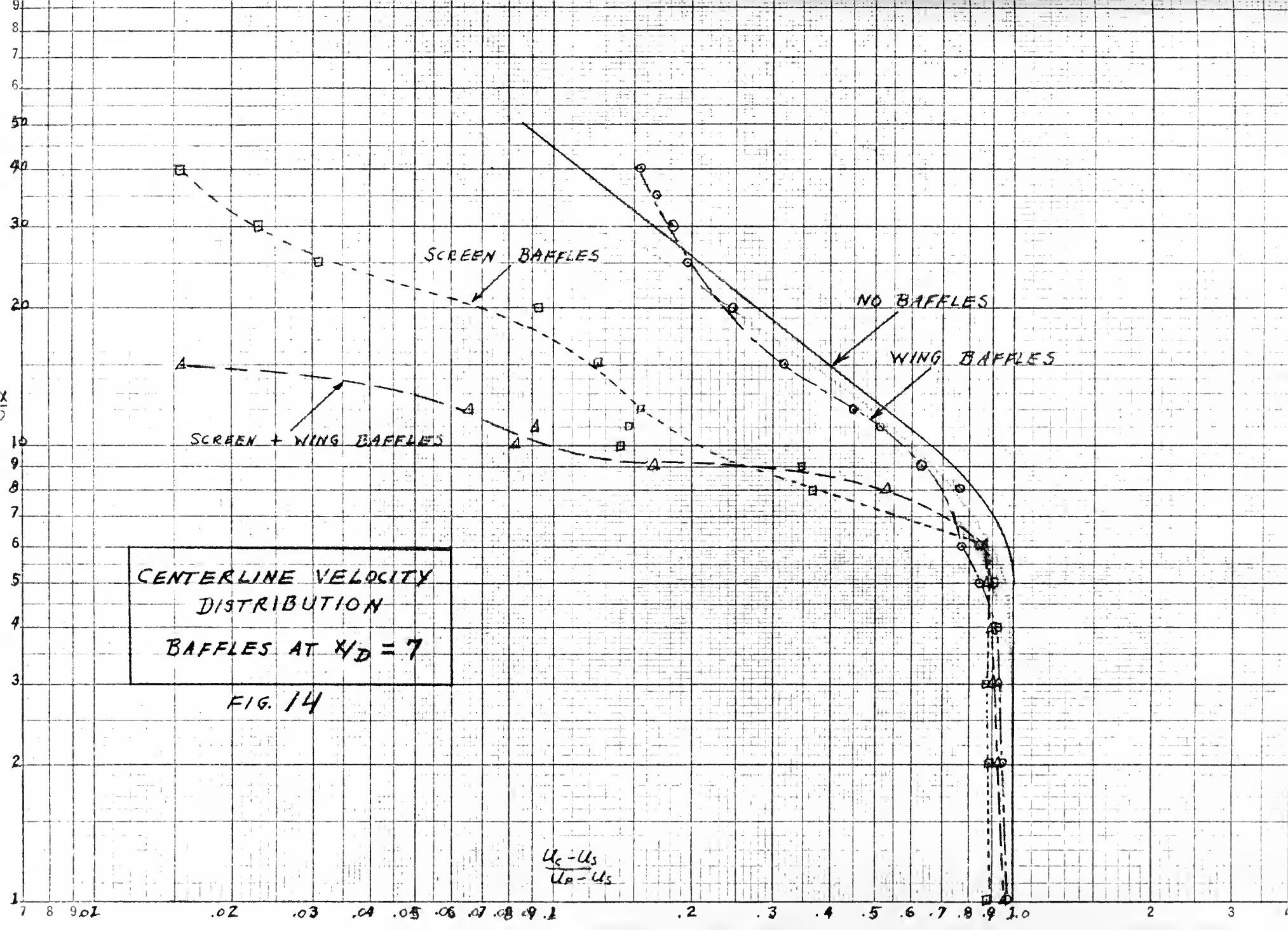
SCREEN BAFFLES
NO BAFFLES
WING BAFFLES
SCREEN + WING BAFFLES
CENTERLINE VELOCITY DISTRIBUTION
BAFFLES AT X/D = 7
$\frac{U_c - U_s}{U_p - U_s}$

FIG. 14

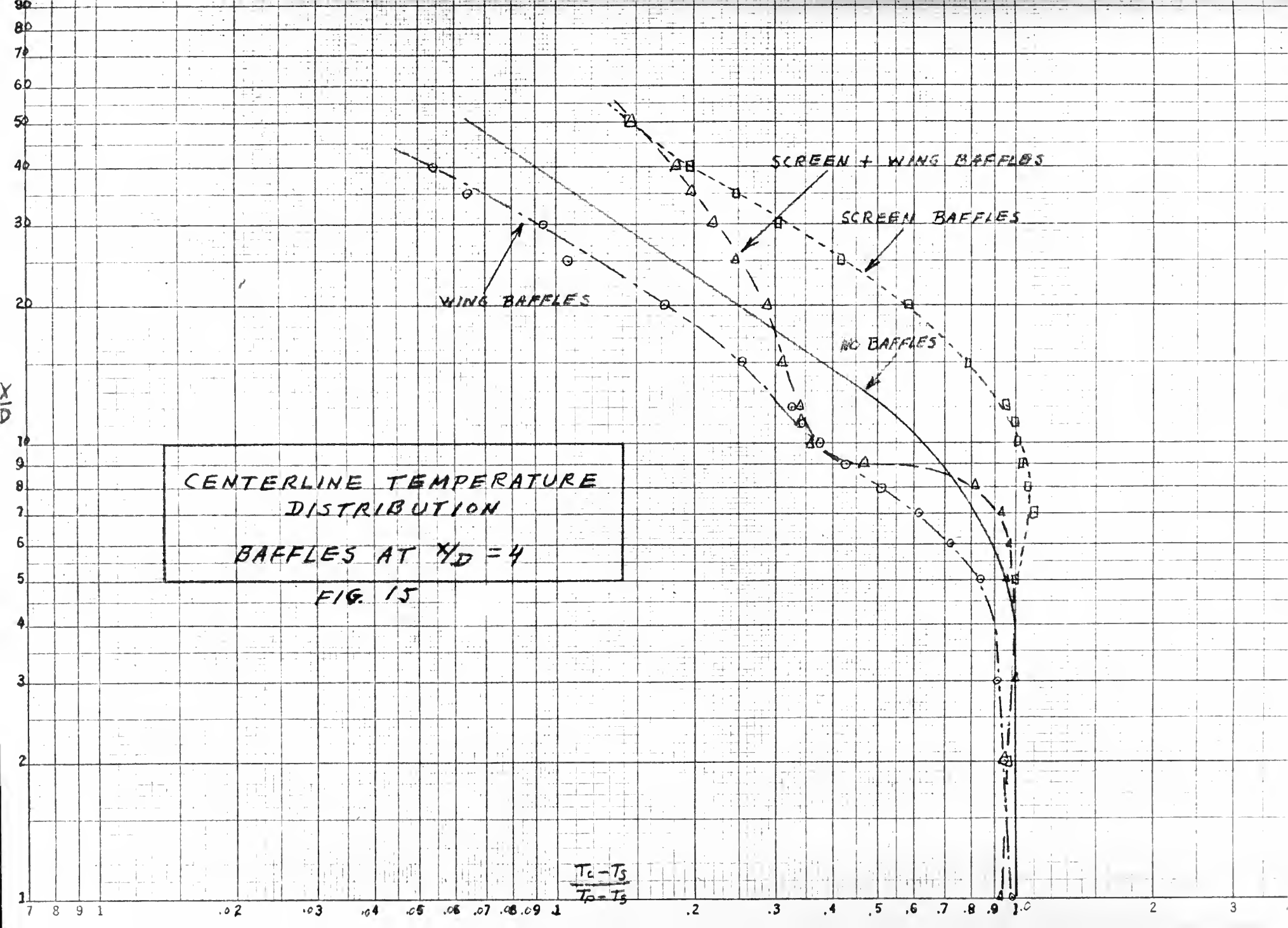

CENTERLINE TEMPERATURE DISTRIBUTION

BAFFLES AT $X/D = 4$

FIG. 15

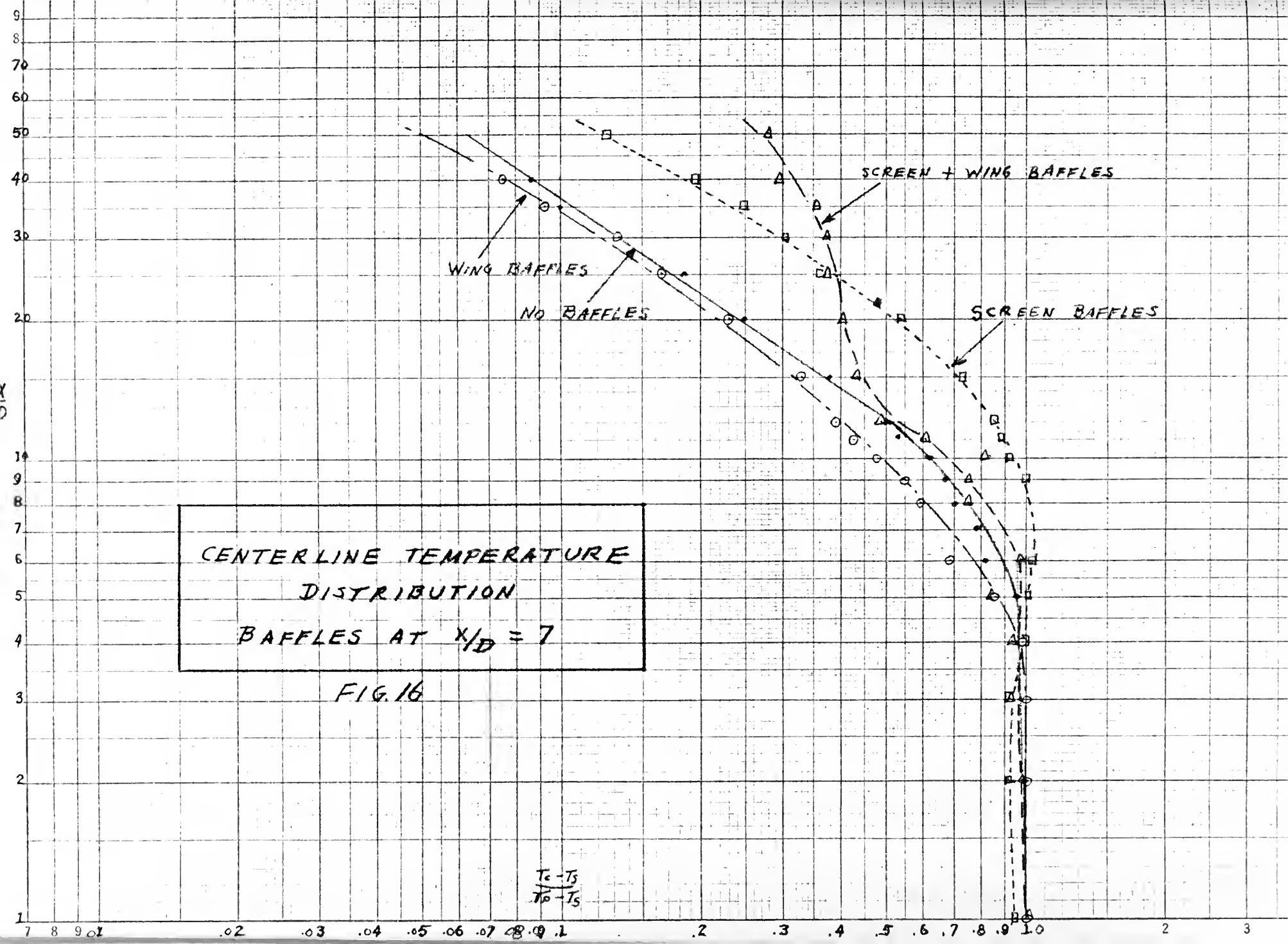

CENTERLINE TEMPERATURE DISTRIBUTION

BAFFLES AT $X/D = 7$

FIG. 16

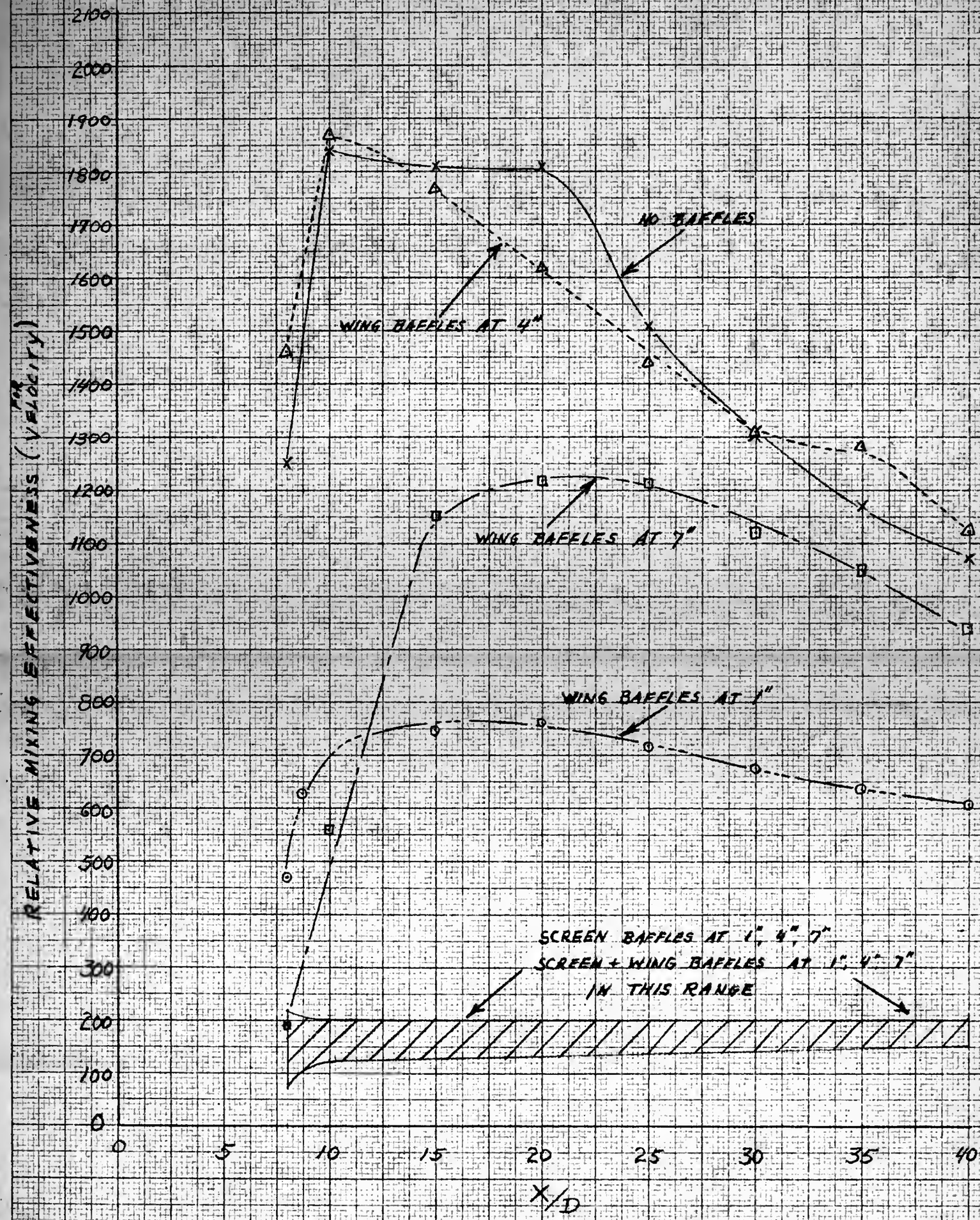

RELATIVE VELOCITY MIXING EFFECTIVENESS VERSUS X/D POSITIONS

FIG 17

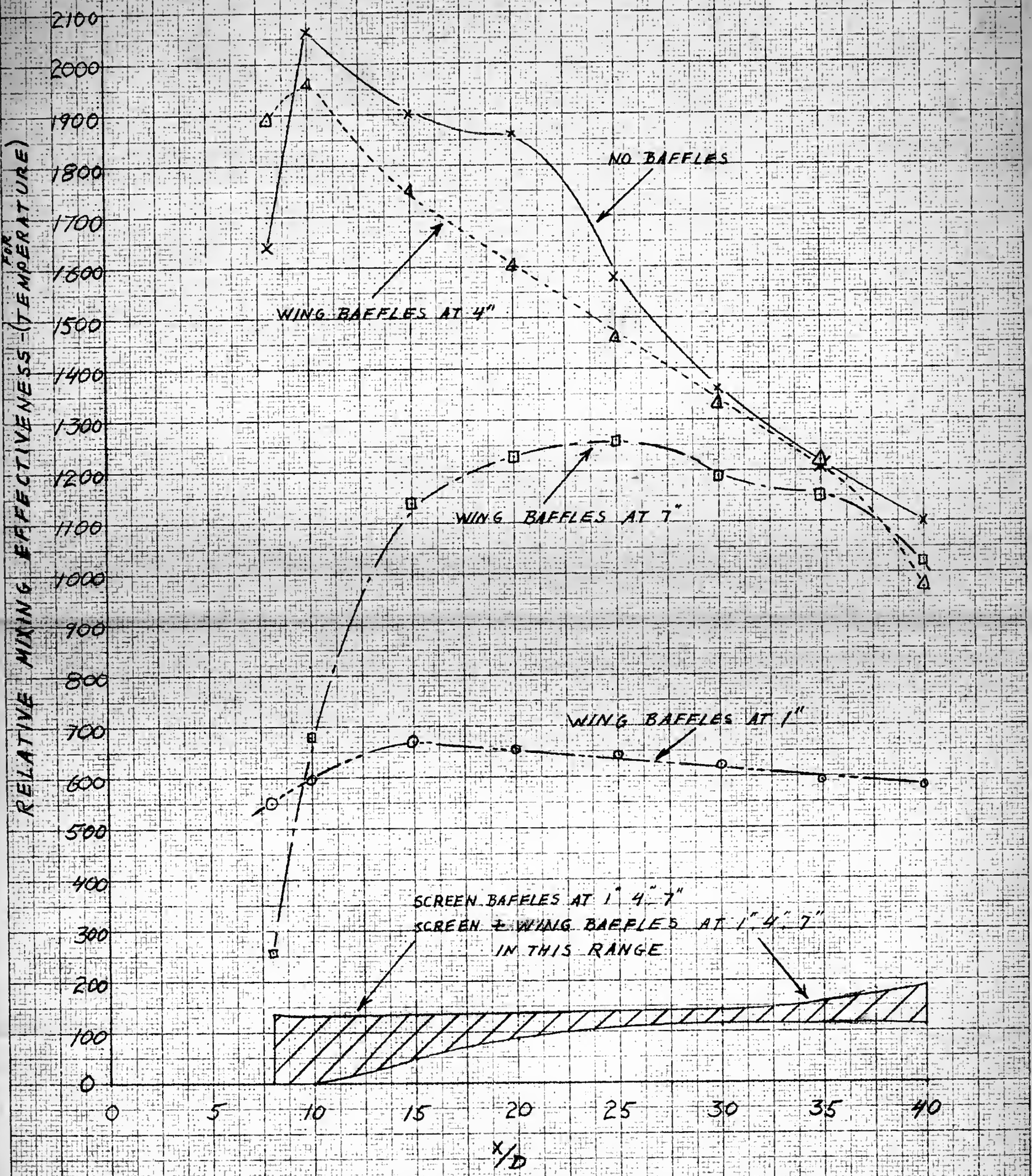

RELATIVE TEMPERATURE MIXING EFFECTIVENESS VERSUS X/D POSITIONS

FIG. 18

TABLE I

MIXING EFFECTIVENESS DATA

X/D	Baffle Location →	Baffles at X/D = 1						Baffles at X/D = 4						Baffles at X/D = 7						No Baffles	
	Baffle Type →	Wings		Screens		Screens plus Wings		Wings		Screens		Screens plus Wings		Wings		Screens		Screens plus Wings			
	Type of Mixing {VEL. = Velocity, TEMP. = Temperature} →	VEL.	TEMP.	VEL.	TEMP.	VEL.	TEMP.	VEL.	TEMP.	VEL.	TEMP.	VEL.	TEMP.	VEL.	TEMP.	VEL.	TEMP.	VEL.	TEMP.	VEL.	TEMP.
8	Mixing Pressure Drop: in. H_2O	0.60		3.23		3.03		0.17		2.80		2.89		1.05		1.80		3.05		0.09	
	% Centerline Mixing	47	54	70	10	90	70	38	49	71	0	80	19	30	40	63	0	47	19	19	25
	Mixing Effectiveness	470	540	123	17	178	139	1460	1890	170	0	146	35	194	258	226	0	83	34	1250	1640
10	Mixing Pressure Drop: in. H_2O	0.62		3.25		3.07		0.21		2.89		2.96		0.52		2.80		2.74		0.11	
	% Centerline Mixing	64	61	74	11	91	68	60	63	76	0	91.5	63	43	52	80	8	90	32	34	38
	Mixing Effectiveness	629	598	129	12	176	132	1870	1960	176	0	164	113	562	680	185	18	177	63	1840	2060
15	Mixing Pressure Drop: in. H_2O	0.69		3.37		3.15		0.28		2.97		3.04		0.40		2.95		2.93		0.18	
	% Centerline Mixing	86	77	83	34	98	70	76	75	86	20	98	70	68	67	88	29	98	56	60	63
	Mixing Effectiveness	747	670	140	57	185	133	1770	1750	194	45	171	122	1155	1140	192	63	181	104	1810	1900
20	Mixing Pressure Drop: in. H_2O	0.77		3.42		3.21		0.34		3.00		3.09		0.43		2.98		2.95		0.24	
	% Centerline Mixing	98	84	98	53	98	73	84	83	91	41	98	71	77	78	93	47	98	60	73	75
	Mixing Effectiveness	762	652	163	88	182	136	1620	1600	207	93	168	123	1220	1230	202	102	179	110	1810	1860
25	Mixing Pressure Drop: in. H_2O	0.82		3.48		3.27		0.40		3.07		3.14		0.45		3.05		3.01		0.31	
	% Centerline Mixing	98	88	98	69	98	76	88	89	94	59	98	75	80.5	84	97	61	98	61	79	82.5
	Mixing Effectiveness	716	644	161	127	178	138	1440	1460	206	130	165	126	1215	1260	205	129	176	111	1510	1580
30	Mixing Pressure Drop: in. H_2O	0.87		3.52		3.32		0.45		3.12		3.19		0.50		3.13		3.05		0.38	
	% Centerline Mixing	98	91	98	77	98	77	90	91	96	69	98	78	82.5	88	98	70	98	63	84	87
	Mixing Effectiveness	675	626	159	125	176	137	1310	1330	204	147	163	130	1120	1192	203	131	173	111.5	1310	1360
35	Mixing Pressure Drop: in. H_2O	0.92		3.57		3.37		0.50		3.17		3.24		0.54		3.15		3.08		0.44	
	% Centerline Mixing	98	92	98	82	98	80	98	93	98	75	98	80	83.5	91	98	76	98	66	86.5	89.5
	Mixing Effectiveness	638	594	157	128	173	141	1282	1220	206	158	160	131	1050	1150	201	156	172	116	1170	1210
40	Mixing Pressure Drop: in. H_2O	0.97		3.62		3.42		0.57		3.22		3.29		0.61		3.23		3.21		0.49	
	% Centerline Mixing	98	94	98	85	98	82	98	85	98	80	98	82	84.5	92.5	98	81	98	69	88.5	91
	Mixing Effectiveness	607	582	154	134	170	142	1120	970	204	161	158	132	941	1025	198	184	165	116	1075	1100

APPENDIX

SAMPLE CALCULATIONS

1. Mass Rate of Air Flow

The equation used to determine mass rate of air flow, for the primary and secondary orifices, was:

$$W = 0.668\, A_2\, K \Sigma I \sqrt{\rho \cdot \Delta p} \quad \text{(See Ref. 19).}$$

where

W = Mass flow in lb. per sec.

A_2 = Throat area in square inch.

K = Flow Coefficient, based on type of pressure taps, Reynold's Number, pipe diameter, and orifice diameter.

E = Area multiplier for thermal expansion of the orifice plate.

Y = Empirical expansion factor.

ρ = Upstream density of flowing air.

p = Pressure drop across the orifice plate in psi.

For the primary orifice, measuring pressure P in in. Hg., ΔP in in. H_2O, and T in degrees Rankine, the mass flow equation becomes:

$$W = .0734 \sqrt{\frac{P \Delta P}{T}}$$

Similarly for the secondary orifice, the equation is:

$$W = 2.52 \sqrt{\frac{P \Delta P}{T}}$$

2. Velocity Determination

Dynamic pressure, $q = \frac{1}{2} \rho V^2$; expressing q in inches H_2O, pressure p in inches Hg., temperature T in °R, the velocity in ft. per sec., becomes: $u = 15.27 \sqrt{\frac{q \cdot T}{p}}$

3. Dynamic pressure error due to changing duct length:

Given, from experimental determination:

For duct length of 72 inches,

absolute static pressure, at X/D = 10, : 407.6 in. H_2O.

dynamic pressure q, at X/D = 10, : 1.7 in. H_2O.

For duct length of 62 inches,

absolute static pressure, at X/D = 10, : 407.3, in. H_2O.

Find dynamic pressure, q, at X/D = 10.

Equating mass rates of air flow, and expressing velocity in terms of q, and density in terms of p, R, and T, there is obtained: $q_{62}p_{62} = q_{72}p_{72}$, remembering that R, T, and A, cross-sectional duct area, remain unchanged as duct length is changed.

Substituting experimental values for q_{72}, p_{72}, and p_{62}, the dynamic pressure, q_{62}, is: $\frac{1.7 \times 407.6}{407.3} \cong 1.7$ in. H_2O

That is, negligible error is introduced into dynamic pressures and velocities by changing duct lengths.

4. Theoretical pressure drop due to mixing:

From conservation of momentum: $p + \rho v^2 = p + 2q$

Or, in terms of experimental areas in $in.^2$, and letting subscripts 1 and 2 refer to states before and after mixing, subscript p for primary, and s for secondary:

$$(p_1 + 2q_{1s})(1 - \frac{.785}{34.7}) + (p_1 + 2q_{1p})(\frac{.785}{34.7}) = p_2 q_2,$$

Rearranging and simplifying:

$p_1 - p_2 = {}^{2}q_2 - 1.95q_{1s} - 0.045q_{1p}$

Substituting average experimental values for the no-baffle configuration, $q_2 = 1.8$, $q_{1s} = 1.6$, and $q_{1p} = 5.90$, (all in inches of water), and solving for the pressure drop due to mixing,

$p_1 - p_2 = 0.21$ in. H_2O.

5. Reynold's Number Calculation:

$R_e = \frac{\rho V L}{\mu}$, where ρ is density of primary air, upstream of orifice, V is velocity of primary air through primary orifice area, L is diameter of primary orifice, and μ is viscosity $= \frac{3.699}{10^7} \frac{\text{lb. sec.}}{\text{ft.}^2}$

Solving for R_e, the value is 57,000.

This value checks accurately the value found using the chart in Ref. 19.

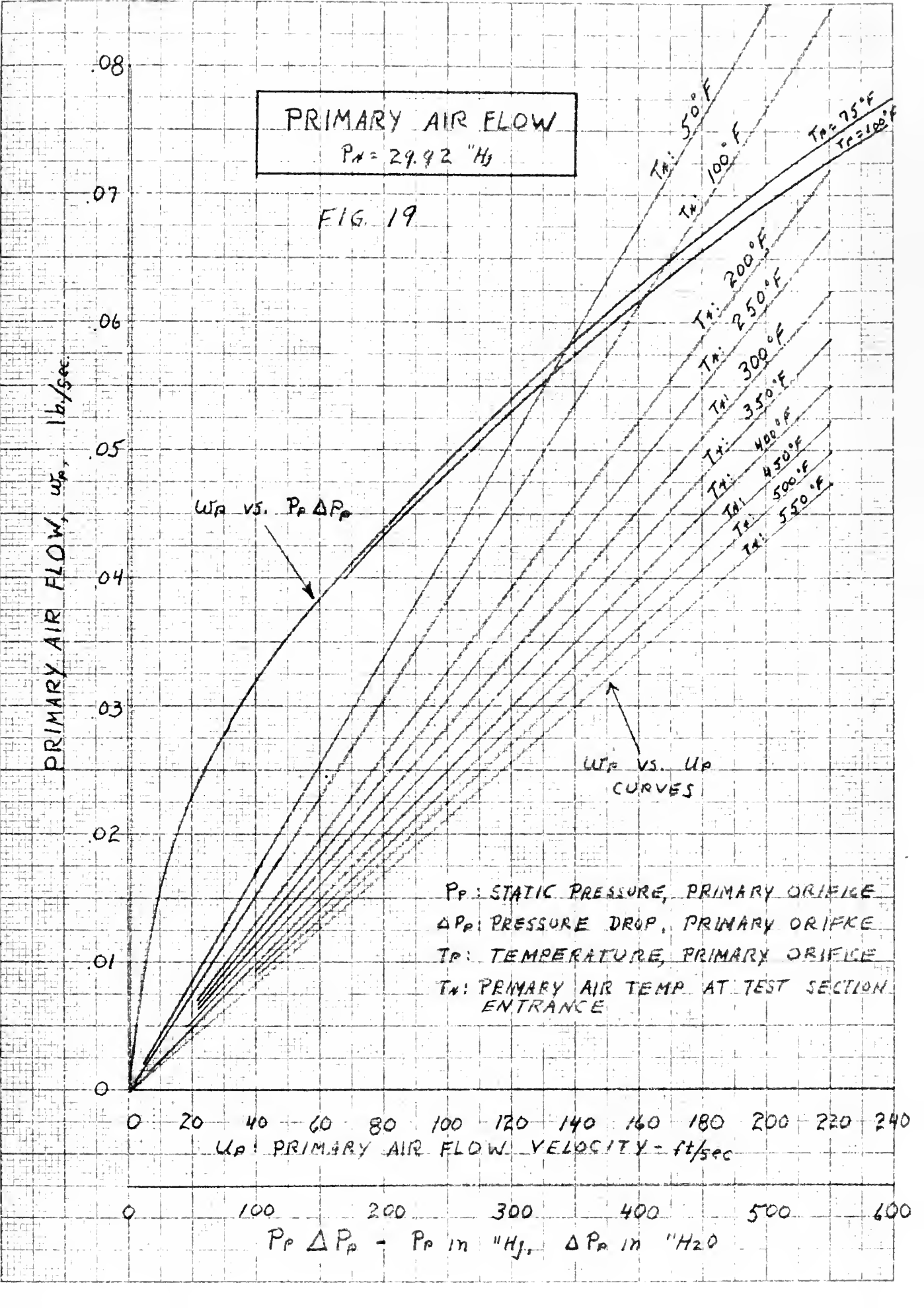
PRIMARY AIR FLOW
P_M = 29.92 "Hg
FIG. 19
PRIMARY AIR FLOW, W_P, lb/sec.
.08
.07
.06
.05
.04
.03
.02
.01
0
W_P vs. $P_P \Delta P_P$
T_M: 50°F
T_M: 100°F
T_M: 200°F
T_M: 250°F
T_M: 300°F
T_M: 350°F
T_M: 400°F
T_M: 450°F
T_M: 500°F
T_M: 550°F
T_M = 75°F
T_M = 100°F
W_P vs. U_P CURVES
P_P: STATIC PRESSURE, PRIMARY ORIFICE
ΔP_P: PRESSURE DROP, PRIMARY ORIFICE
T_P: TEMPERATURE, PRIMARY ORIFICE
T_M: PRIMARY AIR TEMP AT TEST SECTION ENTRANCE
0 20 40 60 80 100 120 140 160 180 200 220 240
U_P: PRIMARY AIR FLOW VELOCITY - ft/sec
0 100 200 300 400 500 600
$P_P \Delta P_P$ - P_P in "Hg, ΔP_P in "H_2O

SECONDARY AIR FLOW

P_N = 29.92 "Hg.

FIG. 20

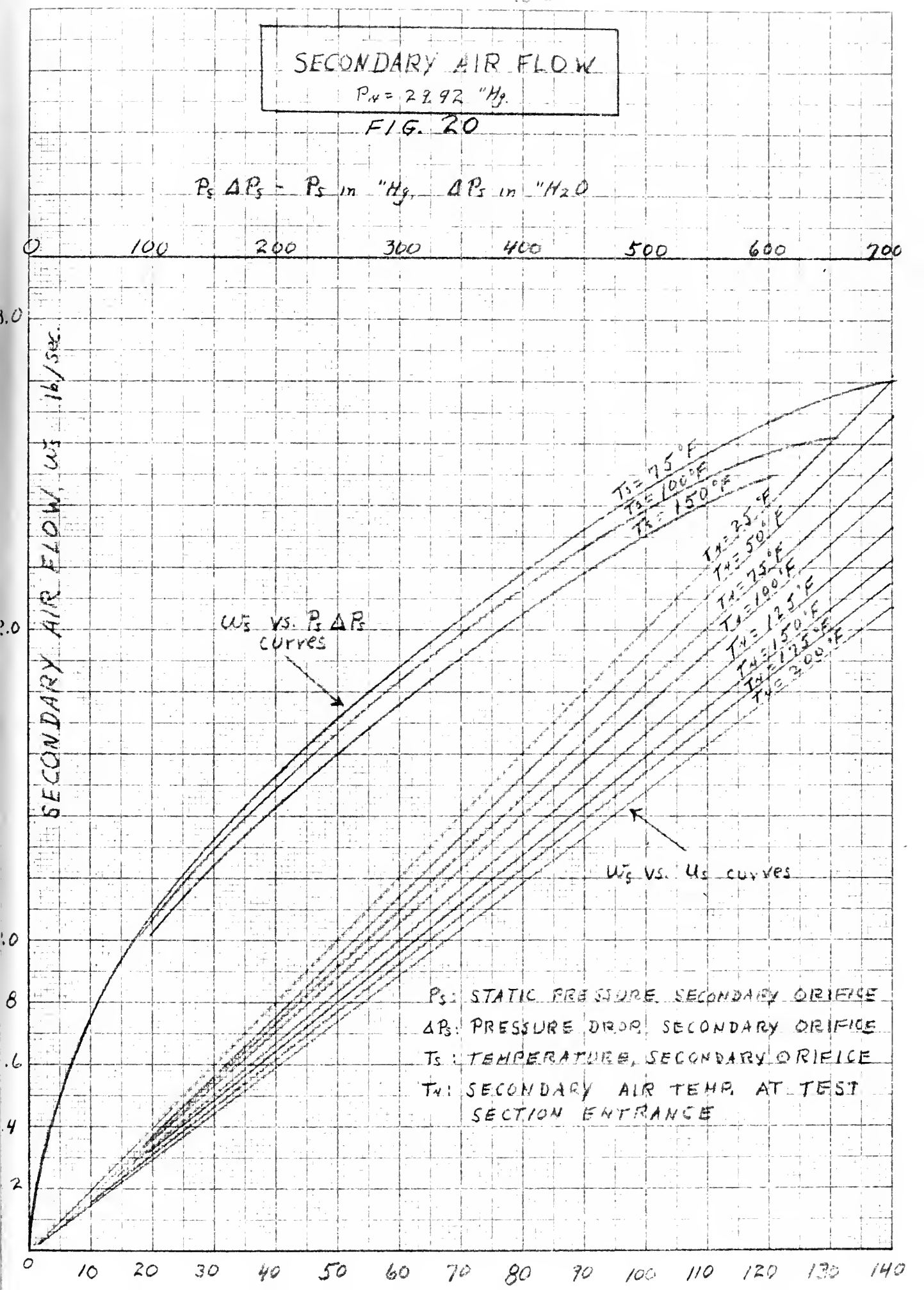

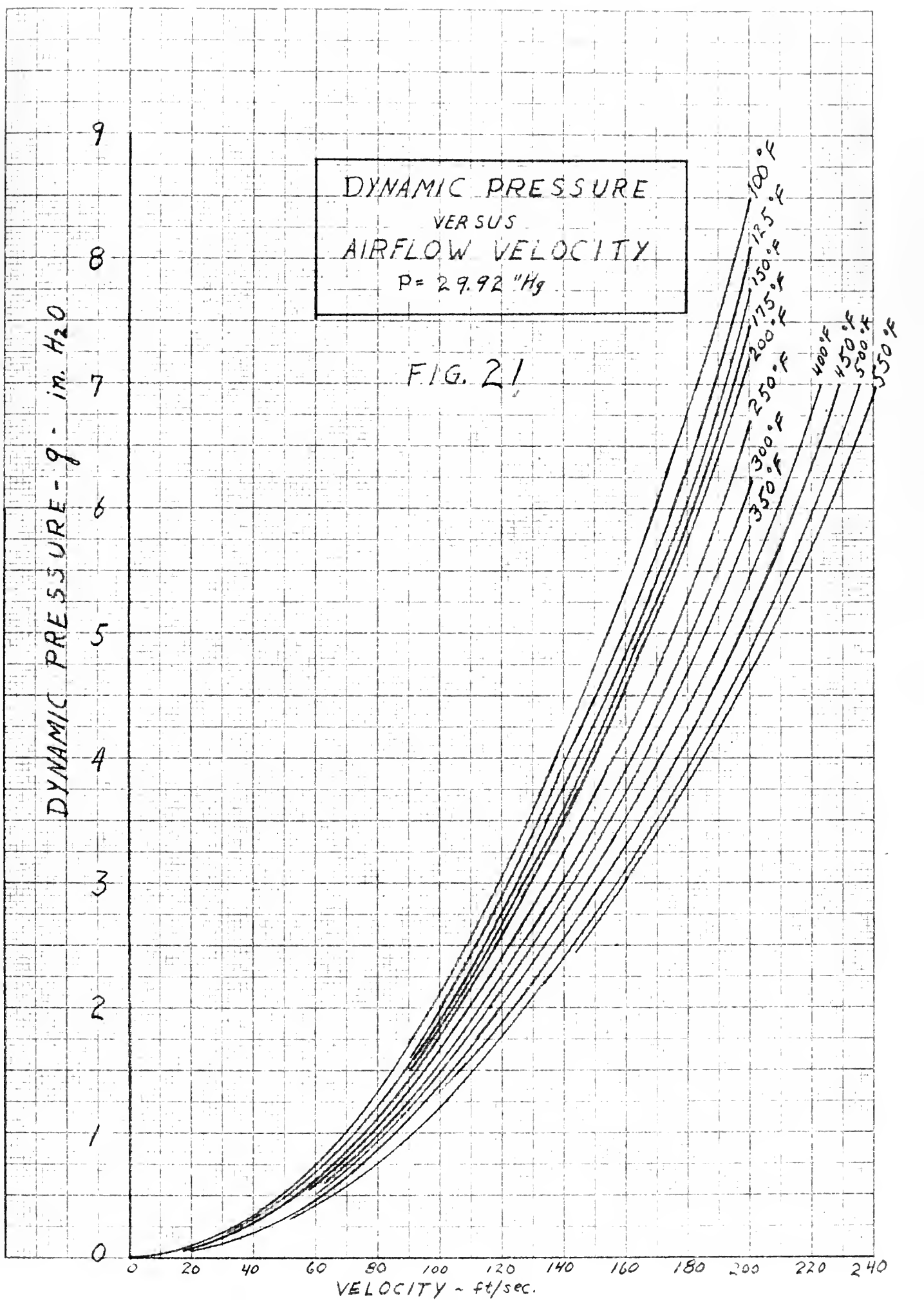
DYNAMIC PRESSURE
VERSUS
AIRFLOW VELOCITY
P = 29.92 "Hg
100 °F
125 °F
150 °F
175 °F
200 °F
250 °F
300 °F
350 °F
400 °F
450 °F
500 °F
550 °F
DYNAMIC PRESSURE - g - in. H2O
0
1
2
3
4
5
6
7
8
9
0
20
40
60
80
100
120
140
160
180
200
220
240
VELOCITY - ft/sec.

FIG. 21

TABLE II

SAMPLE DATA SHEET

TEST CONFIGURATION: NO BAFFLES

BAROMETER*: 29.2 "Hg. ΔP_P*: 6.9 "H_2O T_{P_0}*: 75°F P_{P_0}*: 31.0 "H_g W_P: .0455 lb/sec. VALUES BASED ON MASS FLOWS:

ROOM TEMPERATURE*: 84°F ΔP_S*: 7.2 "H_g T_{S_0}*: 70°F P_{S_0}*: 29.2 "H_g W_S: 1.57 lb/sec. U_P 212 ft/sec λ = .432

STATIC PRESSURE ZERO READING*: 1.14 "H_2O U_S 94 ft/sec

	Units	X/D = 0													X/D = 8											
	Y/D →	0	.2	.4	.5	.6	.8	1.0	1.2	1.4	1.6	1.8	2.0	2.2	0	.2	.4	.5	.6	.8	1.0	1.2	1.4	1.6	1.8	2.0	2.2
q*	in H_2O	5.95	5.85	4.2	3.75	1.15	1.35	1.45	1.45	1.65	1.65	1.70	1.70	1.70	5.3	4.65	3.25	2.85	2.85	1.85	1.6	1.6	1.6	1.6	1.6	1.6	1.6
T_{2-4}*	°F	531	525	520	395	260	270	145	135	130	130	125	125	125	430	440	385	360	320	260	180	135	130	125	125	125	125
T_3*	°F	640	640	640	640	640	650	650	650	650	650	650	650	650	650	650	650	650	650	650	650	650	650	650	650	650	650
U	ft/sec	222	220	187	165	86	92	86	86	91	91	92	92	92	200	190	148	140	137	108	94	90	90	90	90	90	90
		X/D = 12													X/D = 20											
q*	in H_2O	3.75	3.45	2.85	2.55	2.35	1.95	1.75	1.65	1.65	1.65	1.65	1.65	1.65	2.75	2.65	2.55	2.4	2.25	2.0	1.95	1.8	1.75	1.75	1.75	1.75	1.75
T_{2-4}*	°F	345	342	315	290	270	230	190	150	130	125	125	125	125	235	235	225	220	210	195	175	155	140	135	125	125	125
T_3*	°F	650	650	650	650	650	650	650	650	650	650	650	650	650	650	650	650	650	650	650	650	650	650	650	650	650	650
U	ft/sec	160	152	136	127	121	105	98	94	93	92	92	92	92	128	125	122	117	114	106	103	97	95	95	94	94	94
U-Us		69	61	45	36	30	14	7	4	3	2	2	2	2	37	34	31	26	23	15	12	7	5	5	4	4	4
(U-Us)/(Uc-Us)		1.0	.885	.654	.524	.425	.210	.106	.058	.043	.029	-	-	-	1.0	.92	.84	.71	.62	.406	.301	.19	.135	-	-	-	-
r/rm	for velocity	0	.40	.80	1.0	1.2	1.6	2.0	2.4	2.8	3.2	3.6	-	-	0	.286	.572	.715	.856	1.04	1.43	1.72	2.0	2.28	-	-	-
T-Ts		220	217	190	165	145	105	65	25	5	0	0	-	-	110	110	100	95	85	70	50	30	15	10	-	-	-
(T-Ts)/(Tc-Ts)		1.0	.985	.865	.75	.66	.476	.295	.113	.025	-	-	-	-	1.0	1.0	.91	.86	.77	.64	.455	.272	.136	.091	-	-	-
r/rm	for TemR	0	.25	.5	.625	.75	1.0	1.25	1.5	1.75	2.0	2.25	-	-	0	.24	.44	.55	.66	.88	1.1	1.32	1.54	1.76	1.98	-	-

		Y/D = 0																			
	X/D →	0	1	2	3	4	5	6	7	8	9	10	11	12	15	20	25	30	35	40	50
q*	"H_2O	5.95	5.95	5.95	5.95	5.90	5.90	5.90	5.55	5.3	4.7	4.35	4.0	3.75	3.25	2.75	2.4	2.3	2.25	2.2	
T_{2-4}*	°F	531	555	555	545	540	530	470	460	430	415	390	355	345	290	235	210	172	172	167	
U	ft/sec	222	224	224	224	223	223	212	208	199	187	177	166	159	142	126	116	111	109	107	
T_3*	°F	640	670	670	670	670	660	660	650	650	650	650	650	650	650	650	650	650	650	650	
Uc-Us		131	133	133	133	132	132	121	117	108	96	86	75	68	51	35	25	20	18	16	
(Uc-Us)/(Up-Us)		1.0	1.0	1.0	1.0	.994	.994	.91	.88	.812	.722	.646	.565	.512	.384	.263	.188	.150	.136	.120	
Tc-Ts		406	430	430	420	415	405	345	335	305	290	265	230	220	165	110	85	47	47	42	
(Tc-Ts)/(Tp-Ts)		≈1.0	1.0	1.0	.978	.965	.943	.802	.778	.707	.671	.612	.53	.506	.378	.248	.189	.099	.099	.087	
P_H*	"H_2O	1.52	1.65	1.55	1.58	1.58	1.64	1.32	1.35	1.82	1.86	1.50	1.54	1.54	1.48	1.67	1.42	1.53	1.35	1.40	1.30
$P_{H_{corr.}}$	"H_2O	.67	.77	.64	.64	.61	.64	.69	.69	.73	.70	.66	.61	.57	.48	.52	.42	.38	.35	.25	.15

* EXPERIMENTAL VALUES

NOMENCLATURE

T_{2-4} : PROBE TEMPERATURE

T_3 : PRIMARY AIR REFERENCE TEMP

ΔP_P: PRESSURE DROP, PRIMARY ORIFICE.

T_P: TEMPERATURE, PRIMARY ORIFICE

ΔP_S: PRESSURE DROP, SECONDARY ORIFICE

T_{S_0}: TEMPERATURE, SECONDARY ORIFICE

U_P: PRIMARY VELOCITY USED IN COMPUTATIONS = 222 ft/sec.

U_S: SECONDARY VELOCITY USED IN COMPUTATIONS = 90 ft/sec.

Thesis 17335
U24 Ulrich
An investigation of the effectiveness of baffles in promoting mixing of a hot gas with cold air under steady flow conditions.